

9388.

**NASA CONTRACTOR
REPORT**



NASA CR-45

NASA CR-45

164-22015

CODE-1

Oct. 08

**RESEARCH ON A MAGNETO-ACOUSTIC
INFORMATION STORAGE SYSTEM**

by J. W. Gratian and R. W. Freytag

Prepared under Contract No. NASw-592 by
GENERAL DYNAMICS CORPORATION
General Dynamics Electronics
Rochester, New York
for

RESEARCH ON A MAGNETO-ACOUSTIC
INFORMATION STORAGE SYSTEM

By J. W. Gratian and R. W. Freytag

Prepared under Contract No. NASw-592 by
GENERAL DYNAMICS CORPORATION
General Dynamics/Electronics
Rochester, New York

This report was reproduced photographically from copy supplied by the contractor. Its publication should not be construed as an endorsement or evaluation by NASA of any commercial product.

NATIONAL AERONAUTICS AND SPACE ADMINISTRATION

For sale by the Office of Technical Services, Department of Commerce,
Washington, D.C. 20230 -- Price \$2.25

SUMMARY

22015

Solid-state, non-volatile, updatable storage and non-destructive readout are provided by the new delay-line information-storage technique which was studied. Its basic capability for sequential access to data tends toward the low cost, size and weight per bit of information which characterize approaches using traveling storage media such as magnetic drums or tape, but the usual associated mechanical problems are entirely avoided. The technique uses the coincidence of a traveling strain pulse in the line, and a polarizing-field pulse applied to an axial conductor, to accomplish write-in at any prescribed address. Subsequent ultrasonic pulses cause a readout voltage to be induced in the central conductor as they propagate through previously recorded regions.

Study of storage material properties and transducer requirements resulted in the demonstration of operation with one-microsecond pulses using commercial, unoriented, 51 percent NiFe tubing having an OD of 15 mils and a wall thickness of 2 mils. The strain required to accomplish write-in was found to be a major problem. Three primary modes of operation were considered: digital data may be (1) applied to the transducer, or they may be applied as (2) plus and minus or (3) plus and zero polarizing fields. The latter provided the most immediately practicable results using commercially available materials. S/N ratios up to 17 db for 3-microsecond pulses were achieved by special operating techniques using simple magnetostrictive transducers consisting of solenoids surrounding a short portion of the storage medium. The advantages of piezoelectric transducers, however, were found to outweigh their constructional disadvantages for operation with pulses of the order of one microsecond and less. Investigation of parameters using a piezoelectric driver with a horn to provide a 1:10 pressure transformation showed an optimum S/N of 20 db for 3-microsecond pulses and a S/N of 13 db for the calculated maximum available stress without horn coupling.

AUTHOR

Storage materials studied included 8 commercial magnetostrictive alloys of Ni, Fe, Co and Cr. For preferred conditions of operation transverse strain sensitivity, the material property of primary interest, proved to be only a small fraction of the longitudinal strain sensitivity which is emphasized in published data. Explanation of the cause appears to provide a basis for order-of-magnitude improvements in future developments utilizing specially developed oriented materials and thin films.

TABLE OF CONTENTS

SUMMARY	i
1.0 INTRODUCTION	1-1
2.0 MODES OF OPERATION	2-1
3.0 MODEL STUDIES	3-1
3.1 Approach and Materials Considerations	3-1
3.2 Prior Development	3-2
3.3 Resonant Line	3-4
3.4 Piezoelectric Transducers	3-8
3.5 Storage Materials	3-10
3.6 Noise Reduction and Bias Techniques	3-10
3.7 Writein Sequence	3-13
3.8 Single vs. Repetitive Writein	3-14
3.9 Tests of Model With Piezoelectric Driver	3-16
4.0 MATERIAL PROPERTIES	4-1
4.1 Relation of Prior Work	4-1
4.2 Signal-to-noise and Output Criteria	4-5
4.3 Signal Stability	4-7
4.4 Initial Material Studies	4-8
4.5 Advanced Materials Analysis	4-28
5.0 CONCLUSIONS	5-1
6.0 RECOMMENDATIONS	6-1
APPENDIX I REFERENCES	A-1

LIST OF ILLUSTRATIONS

Figure No.	Title	Page
SECTION 1		
1.1	B-H Characteristic for Magnetostrictive Material with no Stress Applied ($\sigma = 0$) and with Stress ($\sigma = k$)	1-2
1.2	Magnetoacoustic Coincident-Pulse Storage	1-2
SECTION 2		
2.1	Magnetostriction Line Waveforms	2-2
SECTION 3		
3.1	Resonant Line Model	3-5
3.2	Effect of Stress on the Saturation Magnetostriction of 50 Permalloy	3-5
3.3	Test Circuit for Resonant Line Model	3-7
3.4	Model with Piezoelectric Horn-coupled Driver	3-9
3.5	Noise Reducing Effects of Bias	3-12
3.6	Effects of (H, σ) Sequence on Output Level	3-13
3.7	Effect of "Creep" in Magnetization as function of Polarization Level	3-15
3.8	S/N and Pulse Density Using 0.1" Thick Ceramic Driver and Horn Assembly with Non-biased Repetitive Writein	3-18
3.9	Results of High Resolution Transducer	3-19
3.10	Test Circuit for Model with Piezoelectric Driver	3-20

LIST OF ILLUSTRATIONS (Continued)

Figure No.	Title	Page
SECTION 4		
4.1	Material Sample Assembly and Bonding Fixture	4-9
4.2	Test Apparatus	4-9
4.3	Magnetization Curves for Annealed Nickel	4-11
4.4	Magnetization Curves for Annealed NiFe	4-12
4.5	Magnetization Curves for Annealed NiFeCr	4-13
4.6	Magnetization Curves for Hard-Drawn NiFe	4-14
4.7	Magnetization Curves for Hard-Drawn NiFeCr	4-15
4.8	Strain Sensitivity for Annealed Nickel	4-18
4.9	Strain Sensitivity for Annealed NiFe	4-18
4.10	Strain Sensitivity for Annealed NiFeCr	4-19
4.11	Strain Sensitivity for Hard-Drawn NiFe	4-19
4.12	Strain Sensitivity for Hard-Drawn NiFeCr	4-20
4.13	Write-Read Cycle for Annealed Nickel	4-22
4.14	Write-Read Cycle for Annealed NiFe	4-23
4.15	Write-Read Cycle for Annealed NiFeCr	4-24
4.16	Write-Read Cycle for Hard-Drawn NiFe	4-25
4.17	Write-Read Cycle for Hard-Drawn NiFeCr	4-26
4.18	15 cps Transverse Hysteresis and Magnetization Characteristics for 49% NiFe	4-29

LIST OF ILLUSTRATIONS (Continued)

Figure No.	Title	Page
	SECTION 4 (Continued)	
4.19	Longitudinal vs. Transverse Strain Sensitivity of Positive and Negative Magnetostrictive Materials	4-31
4.20	Induction and Remanence vs. Field Intensity for NiFeCr	4-34
4.21	Induction and Remanence vs. Field Intensity for 50% NiFe	4-35
4.22	Induction and Remanence vs. Field Intensity for 49% NiFe	4-36
4.23	Induction and Remanence vs. Field Intensity for 70% NiFe	4-37
4.24	Change in Magnetization Curves with σ , H Sequence Reversal	4-38
4.25	Write-Read Cycles Showing ΔB to be More Dependent on Writein History than on Final Remanence	4-39
4.26	Signal and Noise Readout for Stress-biased Writein	4-40
4.27	Effect of Differences in Writein Sequences Using Tensile Stress	4-41
4.28	70% NiFe Hysteresis Loops	4-44
4.29	X-Ray Diffraction Patterns for Thin-wall 51% NiFe	4-47
4.30	Photomicrographs of Grain Structure for NiFeCr	4-48
4.31	NiFe Thin-Film Hysteresis Characteristics	4-50

1.0 INTRODUCTION

Magnetoacoustic information storage is a new technique under investigation with the purpose of developing a single versatile storage process providing the following capabilities:

1. Solid-state operation, avoiding the mechanical problems of drums and discs.
2. Serial address, thus simplifying wiring and switching relative to conventional core or thin-film matrices which require multiple connections to each data cell.
3. Non-volatile storage which can be held indefinitely, updated at will and read out non-destructively.
4. Reading rates in the megacycle range.
5. Reduced cost, size and weight relative to conventional memories.

The material properties utilized in magnetoacoustic storage are shown in Figures 1.1A and 1.1B. With stress σ applied, induction for a given applied field H is greater than with stress absent. As shown in more detail in Figure 1B, the application of a field H_1 , with $\sigma = 0$, produces a residual induction B_1 . However, when a stress pulse is applied simultaneously with H_1 , the induction increases so that a residual induction of B_2 exists when H_1 is removed, and this falls to B_3 when both H and σ are removed. When a stress pulse is subsequently applied to a sample in the B_3 state, the induction again increases toward B_2 , and this change of induction can then be utilized to indicate that a bit of information had been stored. Stress applied to an element in the B_1 state, however, produces a relatively small change of induction.

One method of utilizing these properties is shown in Figure 1.2, where the memory consists of a fine tube of magnetostrictive material, a central conductor,

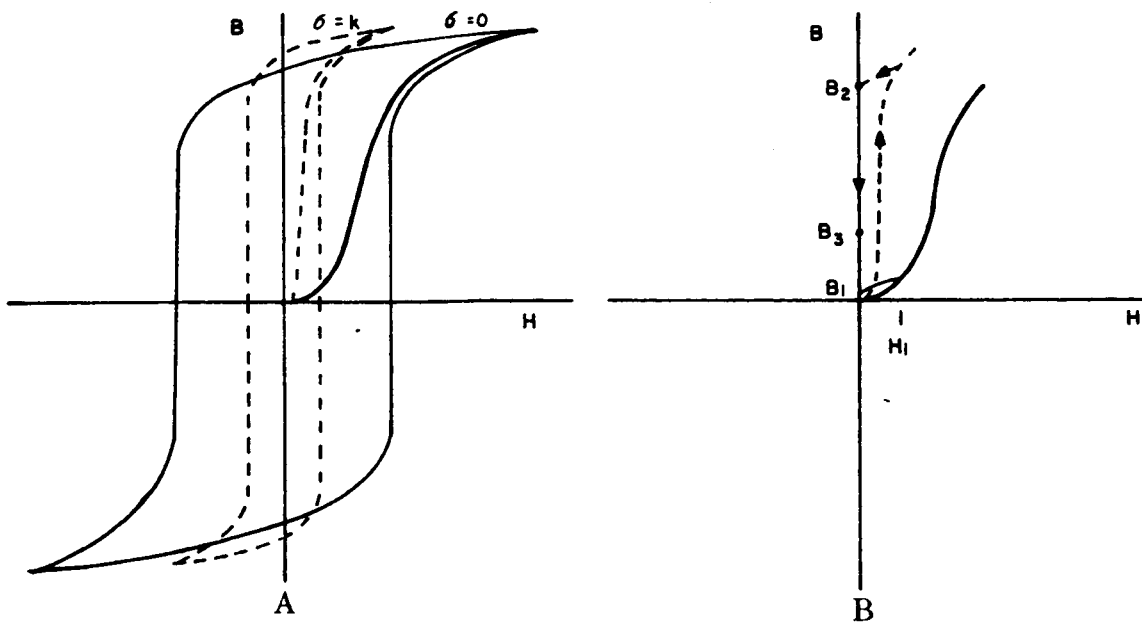


Figure 1.1. B-H Characteristic for Magnetostrictive Material with no Stress Applied ($\sigma = 0$) and with Stress ($\sigma = k$).

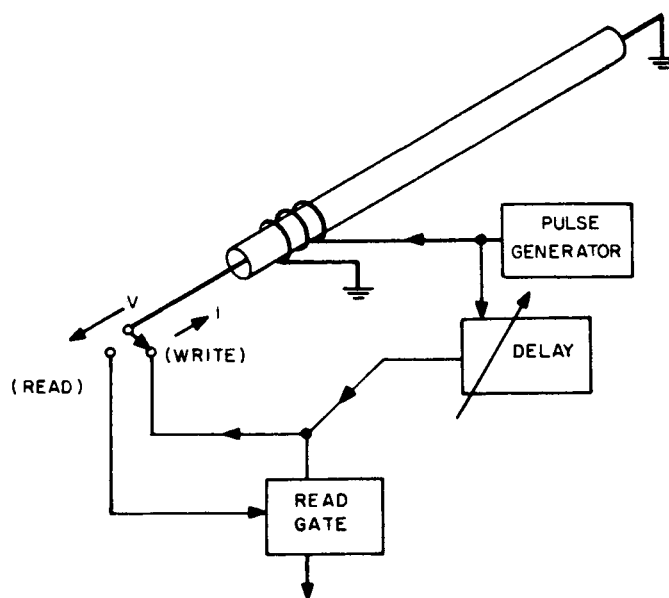


Figure 1.2. Magnetoacoustic Coincident-Pulse Storage.

and an ultrasonic driving transducer at one end of the line. To write, an ultrasonic pulse is first sent down the line. After a delay, which determines the point reached by the ultrasonic pulse, a short current pulse is applied to the central conductor. This leaves an element of the line in the B_3 state of Figure 1.1B. To read, an ultrasonic pulse is again propagated down the line. After a delay corresponding to the address which is to be read out, the gate is opened momentarily, thus providing access to the voltage pulse induced in the central conductor as the passing ultrasonic pulse raises the induction of the addressed element from B_3 toward B_2 . If a ONE is represented by the B_3 state, the B_1 state corresponds to a ZERO. As the readout stress pulse travels through an element of the line in the B_1 state, only a relatively small change of induction and induced output voltage should occur.

For "random-access" applications of the type in which magnetic drums and discs are used, conventional timing or clock circuits would replace the delay circuit of Figure 1.2. When information can be used in serial form, all bits on one line can be read out sequentially as a single pulse travels down the line without need for special timing circuits in the memory. Alternative line configurations envisioned include a solid magnetostrictive wire of small diameter, or a thin-film of magnetostrictive material deposited on a low-loss core material, in place of the tube and axial conductor of Figure 1.2. Alternatives to the mode of operation indicated in Figure 1.1 include switching between states of magnetization of opposite polarity, in accordance with the more widely used conventional digital memory techniques.

Work at General Dynamics/Electronics prior to the study reported herein had demonstrated the basic feasibility of accomplishing both the read and write operations. The purpose of Contract NASw-592 was to conduct research to accomplish improvements in the technique of magnetoacoustic storage. Tasks included evaluation of such materials as nickel, iron, and cobalt; analysis of factors controlling performance; study of configurations, including the potentialities of thin-films; and the construction of models as needed to confirm analyses.

2.0 MODES OF OPERATION

Published papers ^{1,2,3} on conventional magnetostrictive lines show that strain, flux, and output voltage relations under idealized conditions can be represented as in Figure 2.1. A step function of current applied to an ultrasonic driving transducer produces a rectangular strain pulse. A strain pulse of opposite polarity occurs when the transducer current is switched to zero. Readout for the conventional delay line is obtained from a transducer consisting of a section of the line coupled to a permanent magnet on which an output coil is wound. A change of line permeability caused by a passing strain pulse alters the flux through the coil, thus inducing an output voltage. The output waveform is determined by the shape of the strain pulse and the response function for the readout transducer. If both are represented as idealized rectangular functions of distance along the line, the change of flux through the coil is a symmetrical triangular function of time. The output voltage, corresponding to the time derivative of flux, consists of dual-polarity pulses for each of the original strain pulses as shown in the left-hand portion of Figure 2.1. Usually the time duration T_I of the pulse applied to the transducer is made equal to the time T_t for sound to propagate through a length equal to that of the transducer so that the waveforms shown in the right-hand half of Figure 2.1 are obtained.

Similar waveforms can be obtained with the magnetoacoustic technique. If the axial writein current is applied momentarily during propagation of a dual-polarity strain pulse, an image of that strain will be recorded as plus and minus variations of induction relative to the remanence produced by the polarizing field alone throughout the remaining unstressed portion of the line. A subsequent rectangular readout pulse, therefore, will cause both an increase and a decrease

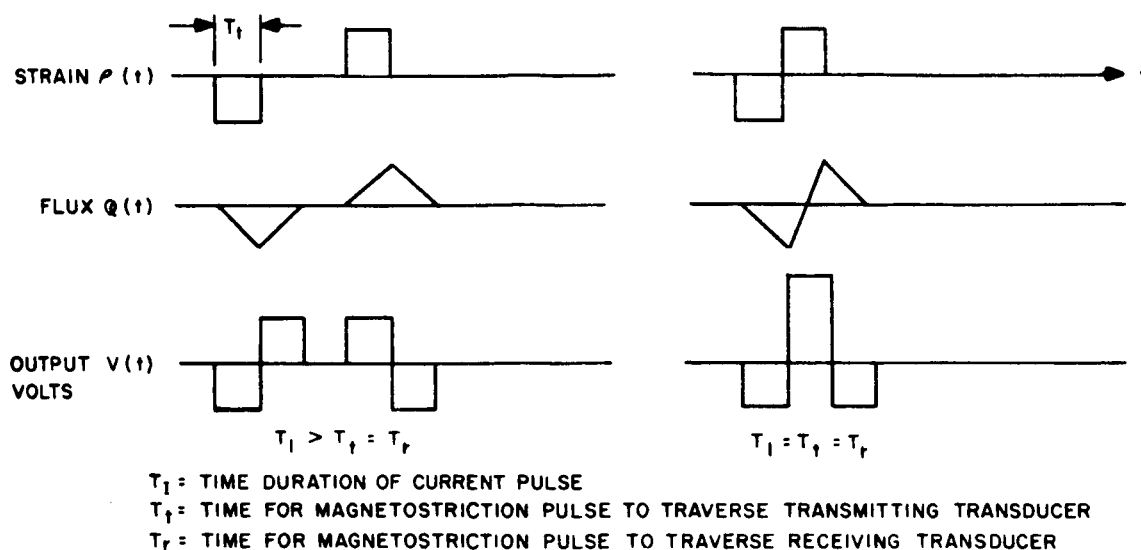


Figure 2.1. Magnetostriction Line Waveforms.

of flux, instead of the simpler change described for the conventional line. Writein current may, however, be maintained as a step-function throughout either a write or read operation, in which case the corresponding strain pulse will be of only one polarity, and waveforms will be as represented in Figure 2.1. Consequently, unidirectional stresses, i. e., either tension or compression were used in the majority of tests reported herein.

Several possible modes of operation were considered. The various techniques used in magnetic recording of digital data appear applicable to the magnetoacoustic process. These include the conventional return-to-zero, non-return-to-zero, frequency doubling and phase-shift methods⁴. The choice from these techniques

will be determined primarily by applications requirements. Three alternative modes of operation, however, are dependent upon special characteristics of the magnetoacoustic process and the properties of materials which can be provided. These are:

1. The data signals may be applied as axial polarizing currents in the form of positive pulses to represent ONES; absence of a pulse then represents a ZERO.
2. The data signals may be applied as axial currents in the form of positive and negative pulses to represent ONES and ZEROS respectively.
3. The data signals may be applied to the transducer to generate strain pulses representing the data; the current pulse applied to the line axis may then be of fixed polarity. This produces modulation of a unipolarity remanence similar to that for Mode (1), and conclusions for Mode (1) are generally applicable to Mode (3) operation.

Mode (2) is preferred because it permits random access updating and provides erasure and rewrite simultaneously without the intermediate erase operation required by Mode (1). Mode (2) offers the greater applications versatility and is more compatible with current data-processing techniques, but on the basis of present materials data it appears more difficult to achieve. Suppose a series of ONES recorded with a positive axial current, and ZEROS recorded with a negative axial current, exist along the line. To change a ONE to a ZERO, a negative axial current pulse is applied to the whole length of line. The site being updated reverses more easily than other addresses along the line because a coincident stress pulse occurs only at that site. However, a substantial unwanted change in remanence at other addresses is usually observed. As will be shown, there is a substantial difference in the capabilities of materials in that respect.

Mode (1) involves two different problems. First to be considered is signal-to-noise ratio. Unless very high stresses are used, which may require excessively costly transducers, an appreciable remanence (corresponding to point B_1) of Figure 1.1B is recorded for ZERO data signals. Since the storage medium is not perfectly uniform, subsequent passage of a readout pulse may generate a noise voltage which is comparable with the signal level. Secondly, the magnitude of the readout signal is dependent upon the difference between the strain sensitivities for the B_3 and B_1 states. That is, assuming a perfectly uniform medium, a readout stress pulse traveling through a consecutive series of recorded ZEROS, corresponding to the B_1 remanence, will produce some increase of induction at the point of increased stress, but the output voltage will remain at zero until the stress pulse begins to enter a region in the B_3 state; a net change of induction then results from the higher strain sensitivity associated with the higher remanence of the B_3 state. The output level as well as the S/N therefore depends upon the relative magnitudes of the strain sensitivities of the two states rather than the induction or strain sensitivity of the B_3 state alone.

The investigation of memory models under dynamic conditions, as reported in the following section, was concentrated primarily on Mode (1) operation using a line of 51 percent NiFe, the most suitable alloy found to be commercially available in thin-wall tubing. Those tests show the effect of variations in media uniformity, as well as operating levels, on S/N. Both Modes (1) and (2), however, were simulated in studies of the static and low-frequency material properties of initial basic concern in magnetoacoustic storage. Results of the materials study provide a basis for substantial future improvements beyond the characteristics of present models.

3.0 MODEL STUDIES

3.1 APPROACH AND MATERIALS CONSIDERATIONS

The three primary objectives of this portion of the magnetoacoustic storage study were as follows:

1. To demonstrate improved practicable model performance as quickly as possible using available commercial materials.
2. To develop a laboratory instrument for the acquisition of the dynamic data needed in analysis of approaches for future improvement in modes of operation, driving efficiency and practicability, signal-to-noise, and resolution.
3. To test, under dynamic conditions, the conclusions from concurrent static materials studies which allow more detailed point-by-point tracing of the magnetoacoustic write and read sequences.

Reasons for the tentative selection of materials to be used as storage media are given in Section 4. The choice was based primarily on the relatively high longitudinal strain sensitivity attributed to 50-70 percent NiFe under external polarization. Originally it was presumed that these materials would have similar transverse characteristics. Measurements discussed in Section 4, however, showed transverse strain sensitivity to be relatively small when materials were subjected to stresses in the direction which tends to increase induction beyond the value for zero stress. Consequently, the development of suitable stress levels for writein was found to be a major problem.

Study of techniques utilizing magnetostrictive transducers was emphasized initially because of the constructional simplicity of these devices. Magnetostrictive generation of a longitudinal strain pulse requires only that a current pulse be applied to a small solenoid loosely surrounding a short section of the

storage medium. Piezoelectric transducers, on the other hand, having mechanical impedances different from that of the storage media, must be matched acoustically through some means of transformation. They must also be securely attached to the media through a bonding agent which should have the same mechanical impedance as the media or transducer, be able to withstand large cyclic stresses, and be limited to a very thin layer at the junction with respect to the wavelength. These effects become important at any discontinuity such as a bond which tends to attenuate and disperse the stress wave as the bond thickness approaches that of the wavelength. Ideally, the ratio of wavelength to bond thickness should be at least 100 for bonds whose acoustical impedance is appreciably different from that of either the transducer or media. These problems become increasingly difficult as line diameter is reduced to improve resolution.

Piezoelectric transducers are capable of generating much higher stresses (five times that of a single magnetostrictive transducer employing 52 alloy and three times that for Ni) and shorter wavelengths without limitations imposed by fringing effects, but anticipated improvements in transverse strain sensitivity and material uniformity suggested that simple magnetostrictive transducers might become practicable. Also, the fact that conventional delay lines using magnetostrictive transducers are operated at rates in the 2 to 5 mc range was taken as an indication that comparable rates could be achieved with magnetoacoustic storage. Consequently, magnetostrictive transducers were to be explored carefully before undertaking the development of piezoelectric drivers.

3.2 PRIOR DEVELOPMENT

The initial magnetostrictive driver utilized a coil length of 0.3 inch to avoid resolution limitations. The coil was wound with fine copper wire directly on a 0.020 inch diameter mandrel, potted, and slipped off onto the 0.015 inch diameter tubes. Although mechanically isolated, this still provided close magnetic coupling with the line. Thus, with 200 turns/cm wound in a single layer, 400 milliamperes

peak current yielded a field intensity of approximately 100 oersted. At this field, the magnetostrictive strain and Young's modulus are 37×10^{-6} in/in and 30×10^6 psi for nickel respectively, and 26×10^{-6} in/in and 24×10^6 psi for 52 alloy. The propagated stress, therefore, being half of the statically generated stress, amounts to 550 psi for Ni and 310 psi for 52 alloy. This, however, was found inadequate with both materials, as model tests showed noise levels to be much larger than signal levels.

Although stress levels were adequate for readout, it was necessary to increase the stress substantially for writein. This was accomplished by sequentially pulsing six transducers, each 0.3 inch long, spaced along the line such that the current through the following transducer was not turned on until the stress pulse generated by the first coil lay directly under the next transducer. Approximately 12 db S/N could be obtained with five reinforcements and about 1 db S/N with only one reinforcement. The pulse widths of H and σ were approximately 2.6 microseconds each, producing an output pulse width of about 8 microseconds. These results were obtained under direct record conditions and could be improved to 10 db S/N with post bias and one reinforcement as discussed in Section 3.6. The coil length was later reduced to 0.125 inch and corresponding input pulse widths to 0.8 microseconds. The results showed a negative S/N ratio with one reinforcement even with bias. Another sample of 52 alloy, annealed for four hours at 2100°F in a dry hydrogen atmosphere and cooled at a rate of less than 100°F per hour, was also tested. Using six transducers and five reinforcements again, the results revealed a signal level below the noise level.

A more practical approach was the development of a resonant line which increased the stress to 1500 psi in 52 alloy using only a single transducer to reinforce the reflections from the undamped ends of the line. With a coil 0.125 inch long and corresponding input pulse widths equal to 1.3 microseconds, approximately 6 db S/N was obtained under biased conditions, although low-frequency components of the stress pulse tended to distort the pulse shape. Differentiation and clipping

of the output waveform, however, produced pulses which could be packed as close as 5 μ sec with 10 db S/N. All figures given above for S/N ratios and resolution were obtained by repetitively recording at the same spot on the line as described in Section 3.8. Electrical connections were made to the line itself, rather than a central conductor, for both writein and readout. Single writein using reset pulses, and attempts to update sections of the line, were only moderately successful. Initial work on a third approach included analysis, design, and construction of conical horns for use with piezoelectric transducers.

3.3 RESONANT LINE

The resonant line which was able to achieve the same stress amplitude as a direct coupled piezoelectric driver without introducing additional variables peculiar to bonded transducers was investigated further in the work to be reported below. A photograph of the model tested is shown in Figure 3.1. Basic construction consisted of placing a short 0.1 inch-long coil at the center of a 12-inch length of magnetostrictive tubing of low acoustical attenuation. A single central copper conductor was threaded through the tube and pulled taut between two damping pads, and thus served both to support the line and to carry the magnetization current. Since the position of the coil transducer was fixed with respect to the chassis, the storage tube could be moved along the central conductor until the coil was accurately positioned, within a few mils, at the center of the tube. This positioning of the tube was aided by the use of micrometer screw adjustments at each end of the line.

As discussed in Section 2, the application of a step input of current to the transducer propagates a unidirectional stress pulse (compressive for 52 alloy) down each half of the line. The pulses are reflected from each end of the line as tensile stress pulses and at some later time merge and lie directly within the coil again. At this time, the current through the transducer is turned off, thus reinforcing the tensile stress pulse. This process is continued, alternately re-

inforcing tensile and compressive stress pulse until the acoustic propagation attenuation is equal to the gain in strain as a function of stress in accordance with Figure 3.2. Thus, a unidirectional square wave applied at the proper funda-

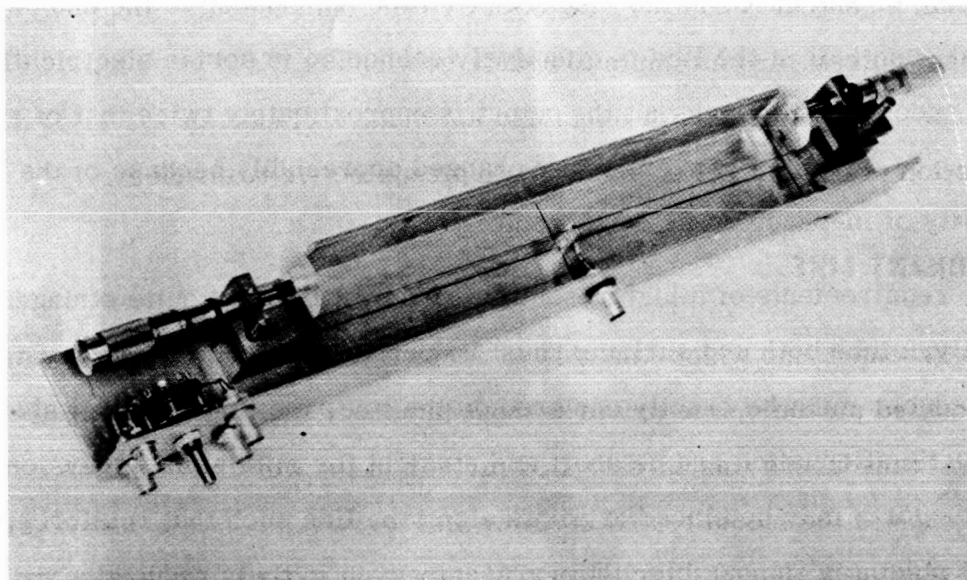
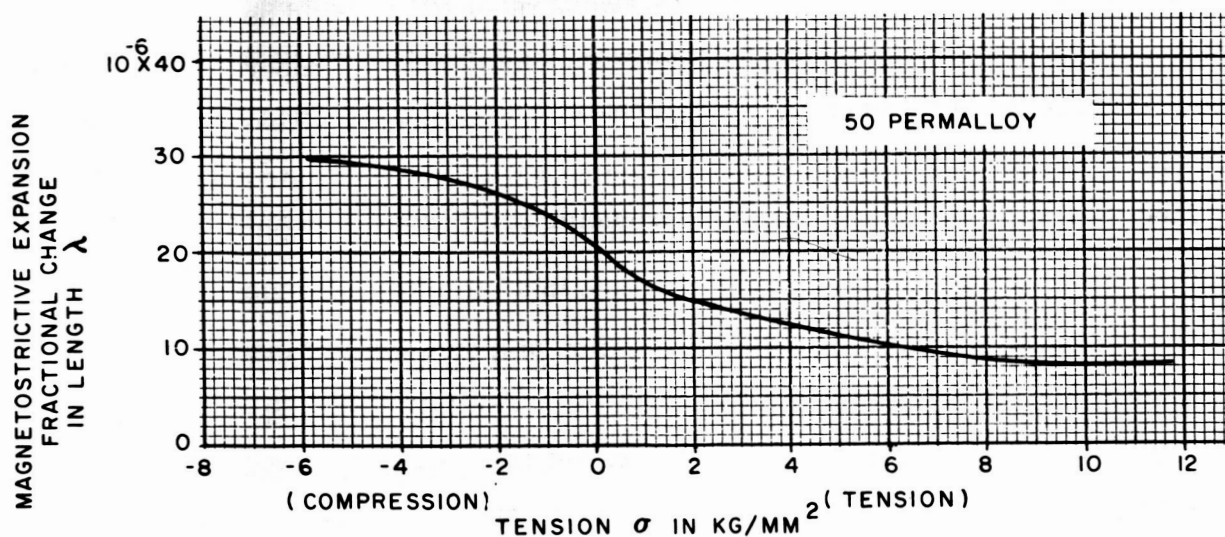


Figure 3.1. Resonant Line Model.



(AFTER R.M. BOZORTH, FERROMAGNETISM, D. VAN NOSTRAND CO., 1951, P. 672)

Figure 3.2. Effect of Stress on the Saturation Magnetostriction of 50 Permalloy.

mental frequency continuously propagates large amplitude stress pulses of alternate polarity in opposite directions along the line either toward or away from the transducer. The cycle time for recurring stress pulses of identical polarity and propagation directions is four times the length of the storage medium. The storage length, in this case, is the distance from the transducer to the end of the line. Note that each half of the line is effectively connected in series electrically and in parallel mechanically such that the output is approximately twice that of either half. The S/N ratio, however, is not changed appreciably because of the large probability of in-phase noise components.

The requirements of a high resolution resonant line are quite stringent mechanically; since both end surfaces must be perpendicular to the axis of the line, the transducer must be exactly centered on the line, the line material should have low acoustic attenuation and be short and straight for minimum dispersion. Although supports may be placed at points along the line such that reinforcement of spurious pulses is impossible, their presence even in their reduced state could add appreciably to the noise, especially on readout.

The major problem of holding the square-wave coil current in synchronization with changes in line length due to temperature fluctuations could be avoided by using a self-clocking pulse from another line with the same temperature coefficient to trigger the transducer drive current. The low frequency stress components previously noted could be avoided by suitable placement of supports at odd intervals along the line. Use of ferrite checks around the transducer would yield better resolution, but would waste too much space in a large capacity memory.

Even with these disadvantages, however, a 24 inch long line of standard tolerance 52 alloy with a 0.125 inch long transducer yielded a gain in stress of 5 (1500 psi), a S/N of 10 db and a response of 200 kc under prebiased conditions.

Later operation under "partial resonant" conditions, using a 12 inch long line of close tolerance 52 alloy with a 0.1 inch long transducer, produced a gain in stress of 7 (2100 psi), a S/N of 17 db and a response of better than 300 kc also under pre-biased conditions. The term "partial resonance" in this case, refers to a non-continuous operation where recording is accomplished after the stress has reached its maximum value, at which point the coil current is turned off. This eliminates much of the pulse distortion cited above.

3.4 PIEZOELECTRIC TRANSDUCERS

Another method of generating high amplitude stress pulses was through the use of piezoelectric ceramics. Their maximum non-resonant driving stress is about 1500 psi for PZT-4^{*} and for low duty ratios about the same for PZT-5.^{*} Since this stress is no larger than that obtained with the resonant line, an acoustic transformer with a 1:10 pressure amplification was designed to provide ample stress for testing the materials over a broader dynamic range and at higher frequencies for which acoustic losses are much larger.

Previously completed analyses on the response characteristics of conical versus exponential connectors had indicated appreciably larger peaks and valleys in the impedance characteristics of the exponential connector for the same transformation ratio, although the half-power points on the power transfer characteristics were approximately the same. The response of each connector was based on a fixed pressure amplification and length whereby modifications in the response could be calculated quickly for changes in either the length or amplification. For example, doubling the length of the horn for a given pressure amplification shifted the entire response down one octave, whereas doubling the pressure amplification for a given length accentuated the peaks and valleys without changing their relative

^{*}Clevite Corp.

position. The response of the final design for a six-inch conical horn with a 1:10 step-up ratio was 3 db down at 20 kc and flat above 200 kc. The purpose of extending the low pass characteristics this far was to keep the response of the horns from interfering with the ceramics' own bandwidth limitations. Thus, the combined bandwidth of transducer and horn would be limited primarily by the ceramic itself.

The final design of the horn-coupled piezoelectric driver consisted of sandwiching a 0.1 inch thick PZT-5 ceramic disc between two similar brass horns, each six inches long and 0.115 inch in diameter on the large end. The diameter of the small end of each horn was designed for an acoustical impedance match with 52 alloy tubing on one horn and Ni tubing on the other. This resulted in a small end diameter of 0.0115 inch and 0.014 inch for 52 alloy and Ni respectively. Two small holes 0.004 inch in diameter were drilled in each end about 0.020 inch deep to accept and fix the position of the central conductor. This served as a guide for mounting the tube to the horn. Conductive epoxy was used to bond the ceramic, tube, and central conductor to the horn initially, but these joints were later reinforced with a coating of 2540 epoxy. The effect of these bonds on the response characteristics has not been determined, but it is believed that a closer coupling between horn and tube which could be achieved by brazing would improve the response. Epoxy was used only because of its handling ease and its capability of allowing easy removal and interchange of the various samples without damaging the horn. A photograph of the horn-coupled model with piezoelectric driver is shown in Figure 3.4.

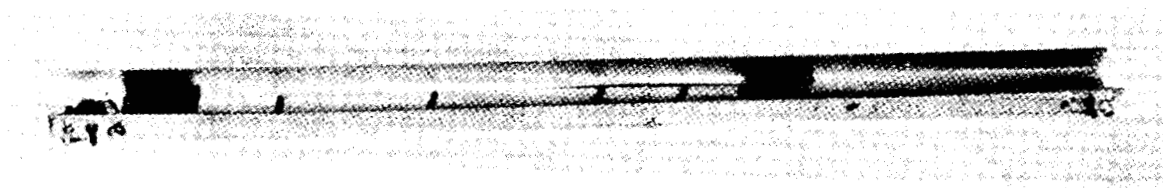


Figure 3.4. Model With Piezoelectric Horn-coupled Driver.

3.5 STORAGE MATERIALS

The materials initially available in configurations suitable for dynamic measurements were "A" nickel, low-carbon nickel, and 52 alloy. These were obtained in 0.015 inch OD tubing with 0.002 inch wall thickness. Tolerances initially were ± 0.0005 inch on the wall and ± 0.001 inch on the OD, but the wall tolerance for later lots of 52 alloy was improved to ± 0.00025 inch. The close-tolerance 52 alloy was received in a hard drawn state, in a mill anneal, and in a final anneal. The mill anneal, according to the supplier, consisted of annealing in a cracked ammonia atmosphere for 1-1/2 to 2 minutes at 1600^oF and cooling in 8 minutes, after which the tubes were straightened and cut to length. Because of the possible deleterious effect of work-hardening the material due to the last operations, part of the order was reannealed without final straightening.

The low-carbon nickel was obtained in the hard-drawn, annealed, and semi-annealed states. The low carbon content in nickel serves to minimize impurity content, thus reducing internal strains and increasing the strain sensitivity. Magnetization curves and hysteresis loops of Figure 4.19 for the annealed material under tensile and compressive loads do show relatively high strain sensitivity in the longitudinal direction.

Samples of thin walled tubing were also annealed, using a tube furnace in the laboratory. Using a dry hydrogen atmosphere and a furnace cool, samples of 52 alloy and low-carbon nickel were annealed at 1600^oF for 10 minutes, and at 2100^oF for one hour.

3.6 NOISE REDUCTION AND BIAS TECHNIQUES

As described in Section 2, the voltage obtained from a readout strain pulse as it passes through a recorded bit is the result of the strain pulse moving from a section of low strain sensitivity (unrecorded portions of the line) to one of higher

strain sensitivity (recorded bit). Assuming a perfectly uniform line, no output should occur until the strain pulse reaches the recorded bit. The materials presently available for the magnetoacoustic storage line, however, are not uniform, and noise is caused by variations in outside diameter, wall thickness, permeability, strain sensitivity, and cross sectional area along the line.

Static tests have indicated that the strain sensitivity under remanent conditions due to the application and removal of H alone is approximately proportional to the remanence. Thus, for a given magnetizing current variations in permeability and variations in mean diameter which affect the magnitude of the magnetizing field result in different levels of remanence as shown in Figures 3.5A and 3.5B. Wall thickness variations affect the total amount of flux that can be changed by a strain pulse and also, being directly related to the cross-sectional area perpendicular to the axis, affect the level of the stress. However, since $\Delta\phi$ increases with thickness whereas stress level decreases with thickness, the two effects tend to be self compensating.

All of the noise sources listed above can be compensated to some extent by the use of either of two magnetic bias techniques similar to the DC bias used in magnetic tape recording. In the post bias scheme, a bit is stored by applying a positive magnetization pulse coincident with a propagated stress pulse at some point along the line and then "biasing" by applying just enough reverse magnetization to return the remanent induction of the non-recorded portion of the line to the origin. The pre-bias method differs only in that bias is applied before the writein which requires a reverse magnetization coincident with the stress pulse. Thus, as shown in Figure 3.5A, the remanent induction of the line after biasing would be approximately independent of permeability if H_c were constant along the line. As indicated in Figure 3.5B, variations in H , due to changes in diameter, tend to be mutually compensating under biased conditions, with the result that variations in final remanence are small. Finally, variations in thickness and strain sensitivity are almost ineffectual in changing $\Delta\phi$ if the induction is essentially zero. The results of using the post bias scheme are shown in Figure 3.5C.

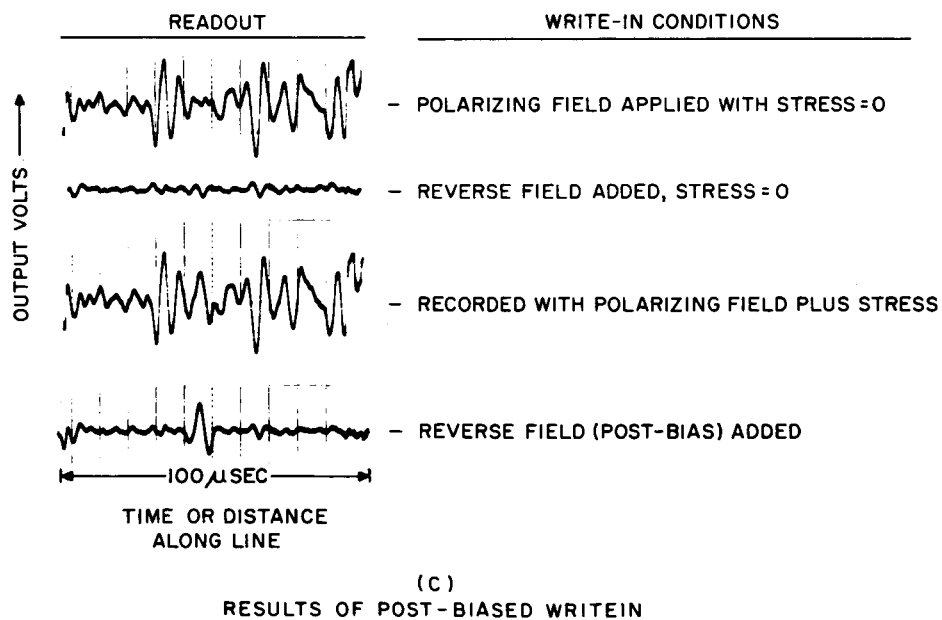
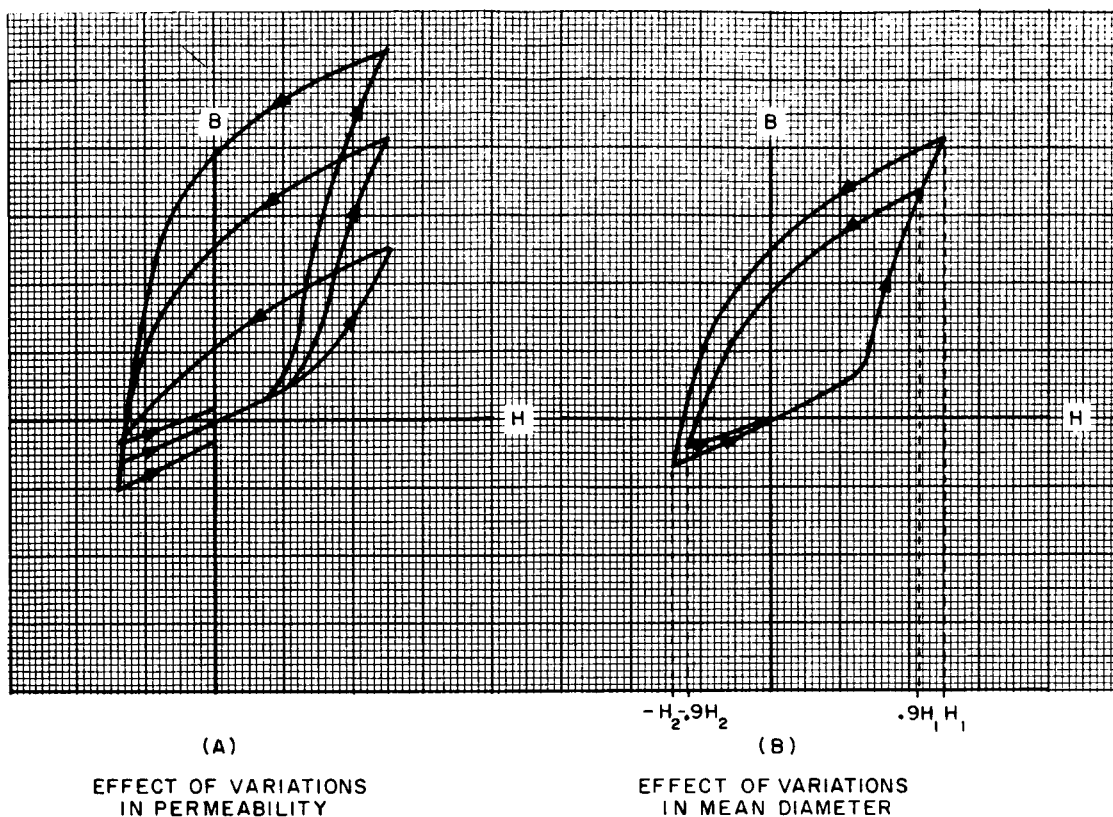


Figure 3.5. Noise Reducing Effects of Bias.

3.7 WRITEIN SEQUENCE

As explained in the introduction, storage of a bit is effected by the coincidence of a σ pulse and an H pulse. Since the σ pulse is in motion when H is applied, as many as three different sections along the line may experience any of four possible sequences of applying and removing both σ and H. Static tests and some dynamic tests have already shown a greater dependency of strain sensitivity Λ on the sequence or history of the writein cycle than the final remanent state. To illustrate, input current pulse widths for σ and H will be denoted by t_σ and t_H . Then for $t_H \ll t_\sigma$, the stress pulse would have barely moved during exposure to the H pulse and would result in effectively only one section or sequence of σ_{on} , H_{on} , H_{off} , and σ_{off} . This sequence will be denoted by $\sigma H \bar{H} \bar{\sigma}$ and is shown in Figure 3.6 with the other three possible sequences dependent upon the duration of the relative pulse widths. Also, shown are the relative output levels as dependent upon the sequence and taken from static measurements on an annealed sample of Carpenter 49 for a given H. The sequence $\sigma H \bar{H} \bar{\sigma}$ is shown as the reference point since the ideal operation for high resolution would exist for $t_H < t_\sigma$.


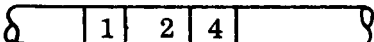
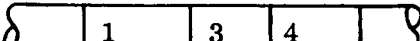
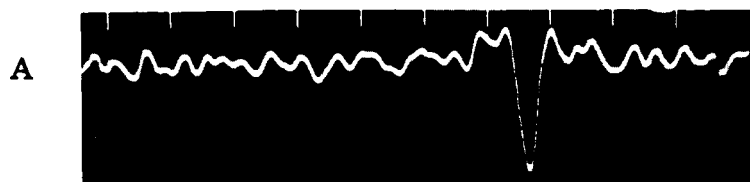
		Section	Sequence	Relative Output Level
$t_H = t_\sigma$	Direction of pulse \rightarrow 	1	$\sigma H \bar{\sigma} \bar{H}$	1.3
		2	$\sigma H \bar{H} \bar{\sigma}$	1.0
$t_H < t_\sigma$		3	$H \sigma \bar{\sigma} \bar{H}$	1.8
$t_H > t_\sigma$		4	$H \sigma \bar{H} \bar{\sigma}$	1.8

Figure 3.6. Effects of (H, σ) Sequence on Output Level.

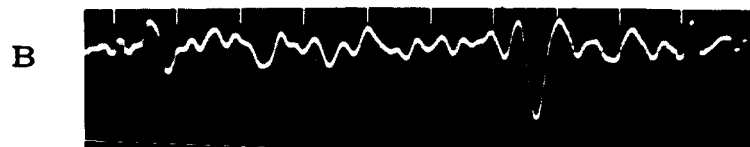
3.8 SINGLE VS. REPETITIVE WRITEIN

Most of the work being reported employed Mode (1), recording either directly or with one of the bias methods. Statically, this consisted of locating an optimum value of H which, following the correct (σ , H) sequence, yielded the largest difference in strain sensitivity between the recorded remanence and the remanence produced by the application of H alone. Consequently, in the initial work which utilized rather broad H pulses, the optimum peak value of H was not far removed from the static condition. With the marginal strain pulses available at the time, considerable improvement in the S/N could be obtained relative to single writein by repetitive applications of coincident H and σ pulses. Using mill annealed 52 alloy recorded with H alone at 2.5 oersteds, strain sensitivity and B_R for a 3 μ sec pulse was found to be 3 db below the values for a DC field. Using coincident σ and 3 μ sec H pulses, output level for single writein was 13 db below that for repetitive writein.

As pulse widths became narrower, higher pulse amplitudes were necessary to maintain the same pulse energy for the optimum single writein H pulse. Continuous pulsing with such a high amplitude H , however, results in a "creep" in the magnetization towards saturation. This destroys data previously recorded and makes it increasingly more difficult to record even repetitively as saturation is approached. Consequently, a compromise between the final remanent state and optimum H amplitude for a given pulse width must be chosen for repetitive writein until ultimately for very narrow pulse widths, the signal-to-noise ratio for single writein is greater than for repetitive. The effect of repetitively applying H pulses without stress over a section of line that had been previously recorded with a single writein is shown in Figure 3.7. Under these conditions, the maximum signal-to-noise that could be obtained is approximately 8 db and is shown in Figure 3.7B. The maximum S/N which could be obtained with a single writein is shown in Figure 3.7C. Further application of H pulses without stress, however, reduces the S/N below 6 db.

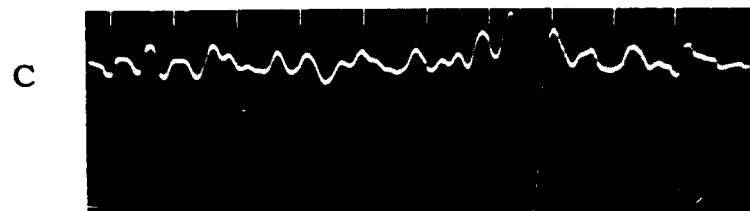


Single Writein.

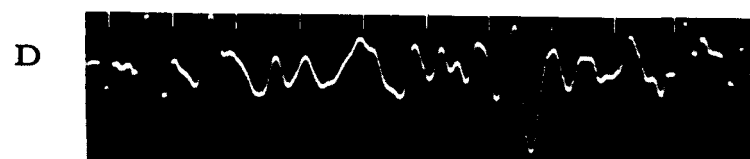


Repetitive H Pulses Applied.

Magnetization Level Adjusted for Maximum S/N After Repetitive H Pulses.



Single Writein.



Repetitive H Pulses Applied.

Magnetization Level Adjusted for Maximum S/N for Single Writein.

Figure 3.7. Effect of "Creep" in Magnetization as function of Polarization Level.

3.9 TESTS OF MODEL WITH PIEZOELECTRIC DRIVER

The mill-annealed close-tolerance 52 alloy was found to be the best available material for the present magnetoacoustic storage model. Cold drawn samples of 52 alloy, Ni and 4 percent CoNi all proved too hard to drive magnetically. A 12 inch long sample of 52 alloy which was annealed in dry hydrogen at 1600⁰ F for one hour was tested in the resonant line fixture but acoustic losses were so great that only a gain of 2.5 in stress could be maintained. Similar acoustic losses were apparent in annealed Ni. Both of the latter samples gave indications of recordings but they were still below the noise level of the line. Later indications of substantial, albeit broad, pulse recordings were produced with the 0.1 inch thick ceramic driver and horn combination using annealed nickel. Because of attenuation and dispersion, output pulse widths were twice as wide as similar recordings made on 52 alloy. Also, the amplitude of the pulses varied considerably along the length of a 12 inch line. Subsequently, all dynamic measurements were confined to the mill annealed NiFe until more data from static measurements, X-ray diffraction studies and thin films become available to guide further dynamic testing of new materials. The following tests on 52 alloy were performed with the 0.1 inch thick ceramic driver and horn assembly except where indicated.

Since a linear relationship exists between the propagated stress amplitude and the input transducer voltage, recorded level and remanent strain sensitivity as a function of the stress amplitude in terms of input voltage, could be measured. Tests showed, in fact, a very linear relationship between stress level and remanent Λ over a broad dynamic range of 26 db with a maximum stress estimated at 3,400 psi. The effect of stress on record level, however, showed a slight non-linearity similar to that of a magnetization curve over a dynamic range of 14 db. Although these recordings were performed repetitively, it is expected that a direct correlation with single writein exists.

Static tests have consistently shown much higher Λ in the direction of decreasing induction as indicated by the magnetization curves. However, simulated recordings on Carpenter "49" using tensile stress showed an even greater dependency on writein sequence than when compressive stress was used. In fact with both $\sigma H \bar{\sigma} \bar{H}$ and $H \sigma \bar{\sigma} \bar{H}$ sequences, the recorded levels for tensile stress were in the same direction as with compressive stress. This was confirmed dynamically by recording with $t_H > t_\sigma$, although the output was some 8 db less than for compressive stress recordings. Likewise, using $t_H < t_\sigma$, recordings of approximately the same amplitude and opposite polarity were obtained in accordance with static tests for $\sigma H \bar{\sigma} \bar{H}$.

Most of the test results on dynamic measurements were based on Mode (1) recordings. Tests have proven, however, the partial feasibility of Mode (2) using either repetitive or single writein. Storage of the initial pulses were only slightly affected by the reverse field and could be stored alternately or in sequence with a pulse spacing of 3 μ sec. Signal-to-noise ratio with both repetitive and single writein also appeared to be improved, in accordance with the expectation that noise should depend only on the uniformity of the record level.

Attempts to update the line using Mode (2) proved unsuccessful. It was discovered that after a bit was recorded, say as a ONE, the coincidence of a negative H with σ was just large enough to return the remanence back to the ZERO level. Thus, a ONE could be changed to a ZERO and back to a ONE again without affecting the amplitude of other recorded bits. Although these tests were performed repetitively, a direct correlation to single writein could be expected.

In summary, tests on the 0.1 inch thick piezoelectric driver and horn assembly provided approximately 25 db signal-to-noise for non-biased repetitive writein. Pulses could be packed as close as 3 μ sec without appreciably affecting the amplitude of previously recorded pulses. These are shown in Figure 3.8. Single writein yielded a maximum of 20 db signal-to-noise, provided no further

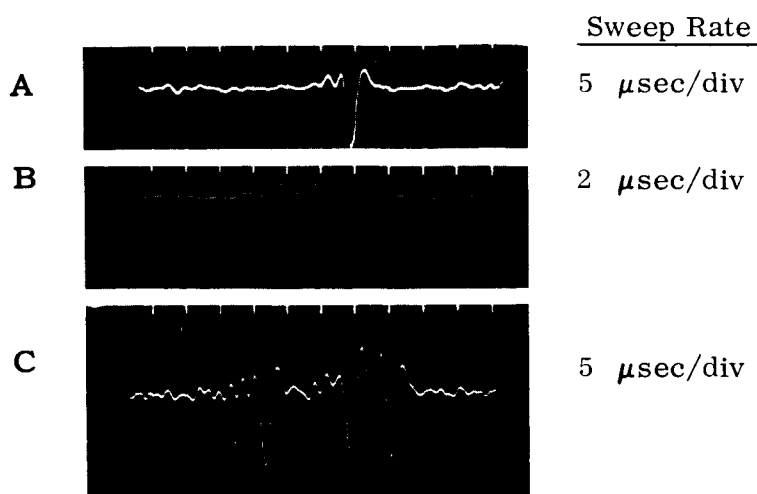


Figure 3.8. S/N and Pulse Packing Density Using 0.1" Thick Ceramic Driver and Horn Assembly With Non-biased Repetitive Writein.

H pulses were applied. This method of recording could be utilized with Mode (3) when the application permits an entire line to be updated at one time. Otherwise, following repeated H pulses, only about 8 db S/N could be expected. The transducer voltage used in these tests was a step input of 1730 Volts/cm peak amplitude and could be increased to 8 KV/cm without depoling the transducer more than five percent at low duty ratios. A direct drive transducer therefore could be constructed and operated at 45 percent of the stress levels obtained with the horn, thus providing 18 db S/N for repetitive writein or 13 db for single writein.

Resolution tests were performed by reducing the thickness (t) of the transducer from 0.1 inch to 0.024 inch using the same PZT-5 ceramic and horn configuration. This transducer was driven with a step input of 7200 volts/cm peak amplitude generating a stress 4 times greater than that used in the 0.1 inch thick transducer experiments. Nevertheless, the output level for $t = 0.024$ inch was 4 db lower than the output obtained with $t = 0.1$ inch for conditions of non-biased single writein and $t_H = t_\sigma$. Using $t_H = 0.5 \mu\text{sec}$, a 15 db S/N and a $1.2 \mu\text{sec}$ output pulse width was obtained for single writein and pre-biased

conditions. This is shown in Figure 3.9A. Likewise for $t_H = 0.12 \mu\text{sec}$, 12 db

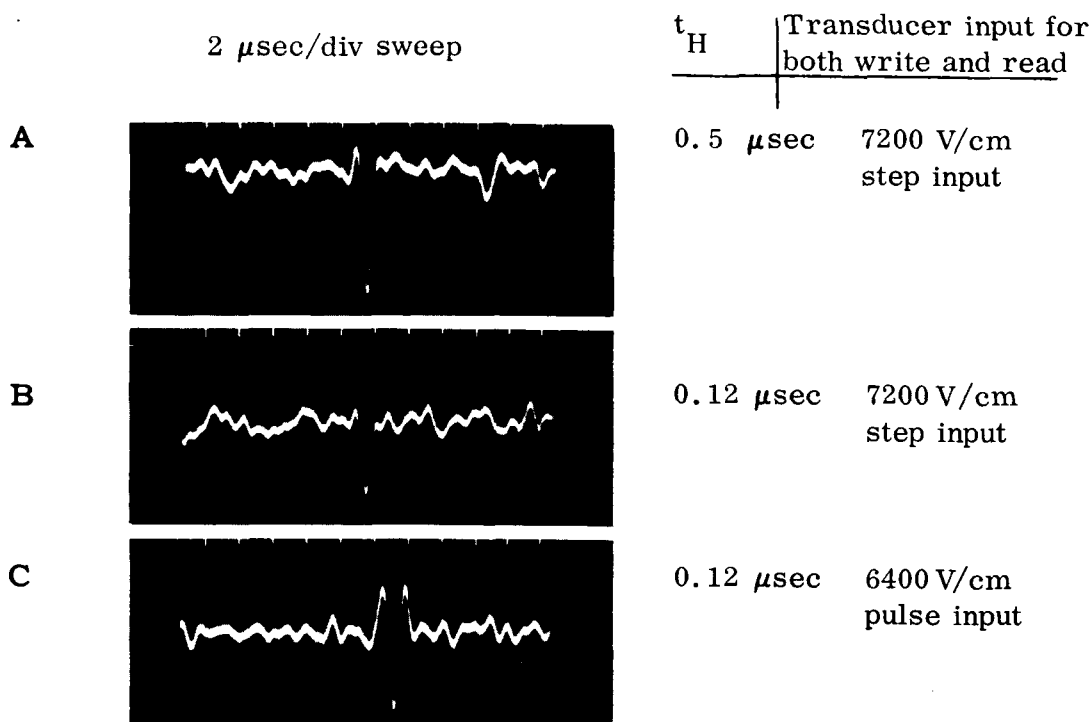


Figure 3.9. Results of High Resolution Transducer.

S/N and a $1 \mu\text{sec}$ output pulse width was achieved as shown in Figure 3.9B. Since repetitive writein actually reduces the signal level and signal-to-noise ratio, Mode (3), which would require a pulse input or a series of pulse inputs to the transducer, would have to be employed. Figure 3.9C shows the output as recorded with a transducer input of 6,400 Volts/cm, $t_H = 0.12 \mu\text{sec}$ and $t_\sigma = 0.4 \mu\text{sec}$. The output waveform as read out with the same transducer pulse input is identical to that obtained with conventional delay lines. The test circuit used with the piezo-electrically driven models is shown in Figure 3.10.

The longitudinal velocity of propagation in 52 alloy tubing is 0.17 inches per microsecond. Hence, one-microsecond resolution provides a linear packing density of 6 bits per inch.

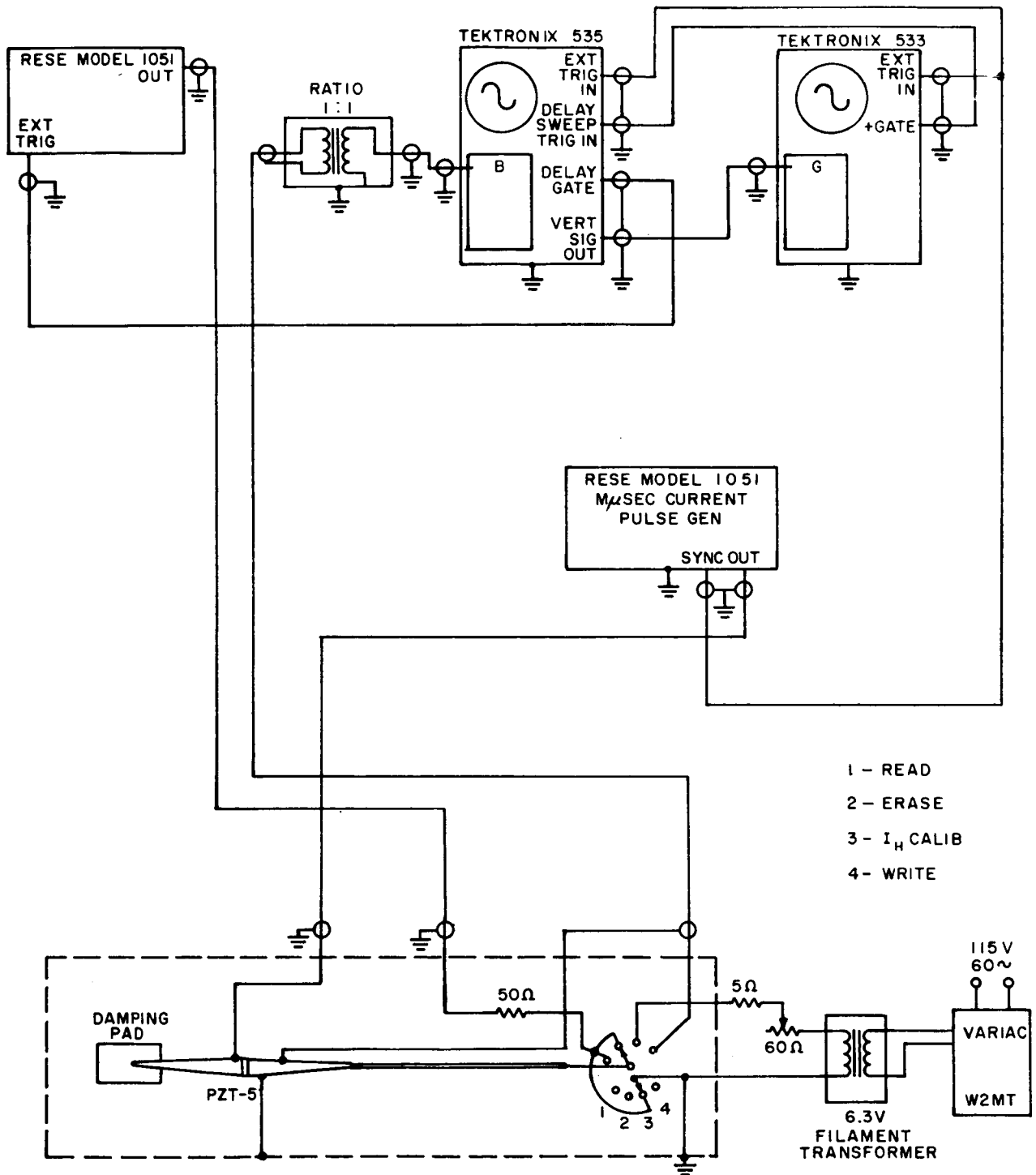


Figure 3.10. Test Circuit for Model With Piezoelectric Driver.

4.0 MATERIAL PROPERTIES

4.1 RELATION OF PRIOR WORK

Published work ¹ on the bulk properties and theory of magnetostrictive materials provides a tentative basis for the selection of materials for magnetoacoustic storage. Data commonly presented are:

1. B-H and magnetization curves at various stresses
2. λ , the magnetostriction, or fractional change of length, versus field intensity
3. Λ , the strain sensitivity, or change of induction per unit stress, versus field intensity or induction

Both the readout and writein processes in magnetoacoustic storage are more dependent upon strain-sensitivity than upon magnetostrictive material properties. This is clearly true of readout. The characteristic utilized in readout, however, is a change of remanent induction rather than the change of induction due to an external polarizing field which is more thoroughly covered in published material. Writein does involve the increase of induction which is produced by a stress in the presence of an external polarizing field, but in this case, it is the remanent induction following the stress, rather than the change of induction during stress which is of interest. Magnetostriction is used in the generation of the stress pulse in the arrangement of Figure 1.2, but this does not require a compromise material; the magnetostrictive transducer can be replaced by an electrostrictive driver, or a material with optimum magnetostrictive properties can be mechanically coupled to a storage line selected for optimum strain sensitivity. Although the two properties are related, maximum strain sensitivity and maximum magnetostriction do not occur in the same material, e.g., ² the strain sensitivity of 68 percent NiFe is much greater than that of Ni, but magnetostriction is greater in 100 percent Ni. The work being

reported, therefore, was concentrated on determining strain sensitivity characteristics under the specific conditions involved in magnetoacoustic storage.

Bozorth and Williams³ have shown that maximum strain sensitivity, when plotted as a function of percent Ni in NiFe, occurs at approximately 60 percent Ni. The maximum is quite broad, and strain sensitivity falls only 25 percent for 50 percent and 70 percent Ni. The early work of Buckley and McKeehan⁴ shows hysteresis loops and magnetization curves for a series of NiFe alloys with and without stress. They provide data for both high and low levels of magnetization whereas the Bozorth and Williams composition optimum refers only to a maximum which occurs at relatively high levels. Of the alloys tested by Buckley and McKeehan, a 65 percent NiFe and a 45 percent NiFe are closest to the 62 percent optimum. The difference between hysteresis loops for stressed and unstressed states appears much greater for the 65 percent NiFe, but a higher stress was used with the 65 percent NiFe and direct comparison is difficult. The magnetization curves again appear to show the 65 percent NiFe more stress sensitive at low magnetization and under more comparable stresses. However, the 65 percent NiFe is much closer to the 62 percent optimum than the 45 percent NiFe, so there is no clear evidence that maximum strain sensitivity at low magnetization is obtained with a different composition than that for high magnetization. Those data, coupled with the fact that 51 percent NiFe was found to be the only alloy in the 50-70 percent NiFe range which was commercially available in thin-wall tubing, led to the selection of 49-51 percent alloys for the most detailed studies undertaken.

It was expected, however, that those data could serve only as a tentative guide to material selection in magnetoacoustic storage for several reasons. First, they pertain to the maximum value of strain sensitivity for each material, and this maximum occurs at a high value of induction. Second, only longitudinal characteristics are treated. Third, an external polarizing field is applied. By contrast, magnetoacoustic storage utilizes transverse characteristics, remanent

polarization, and at least two levels of remanence approached via different H, σ histories.

Longitudinal magnetostriction is the fractional change of length along the direction parallel to an applied field. Transverse magnetostriction is the fractional change of dimension in a direction perpendicular to an applied field. So-called positive materials, such as 50 percent NiFe, show an elongation parallel to the applied field and contraction perpendicular to the field. Positive materials, when polarized, show an increase of induction parallel to an applied tension, a decrease in induction parallel to an applied compression, and reversed effects for the transverse conditions. Each of the above effects is reversed for negative materials such as 100 percent Ni.

Although those relations seem firmly established ⁵, work by Fischell ⁶ has shown that transverse compressional stress applied to clamped laminations of both positive and negative materials has produced a decrease of induction for each of the samples he studied. If this were found true also for the physical configuration used in magnetoacoustic storage, some revision of the process would be required. As described in Figure 1.1, a stress pulse is assumed to cause an increase of induction relative to that of the unstressed medium. According to the commonly accepted relations summarized above, the increase of induction could be accomplished with a positive material and a compressional axial pulse since induction is measured in the transverse circumferential direction. Conversely, a negative material and a tension pulse could be used. If, however, it were found, as in Fischell's measurements, that stress acts only to decrease transverse induction, the storage medium would have to be operated at high induction for zero signal level. This would preclude the possibility of updating — i.e., changing a ZERO to a ONE — without an intermediate erasing operation. It would also require that all data be distributed along the line in the form of strain variations before application of the polarizing pulse, thus precluding random-access writein. Consequently, improved understanding of the seemingly

contradictory published information on transverse strain sensitivity appears essential in the development of magnetoacoustic storage.

The use of induction levels other than that which produces maximum strain sensitivity, and the use of remanent rather than external polarization, introduces additional unknowns requiring evaluation. In magnetoacoustic storage, it is desired to obtain high readout strain sensitivity Λ_3 for the B_3 state of Figure 1.1 but relatively low strain sensitivity Λ_1 for the B_1 state. Bozorth and Williams⁷ show theoretically under idealized conditions that strain sensitivity is approximately proportional to induction at low values of induction and rises to a maximum at an induction equal to 0.6 of the saturation induction. Consequently, it seems reasonable to expect that the maximum ratio Λ_3/Λ_1 should be obtained at a low value of write-in field intensity for which the corresponding remanent induction is relatively small. For larger inductions, Λ_3 would increase less than Λ_1 , thus reducing the ratio. Low recording levels have the additional advantage of low recording power requirements and the disadvantage of relatively low readout voltage. These expectations, however, are based on information for external polarization. In magnetoacoustic storage, change of remanence is utilized during readout and, in addition, there is a basic difference in the previous histories of the B_3 and B_1 states. Whereas B_1 results from an external polarizing field only, B_3 results from external polarization in the presence of strain, so it would not be surprising to find different subsequent strain-sensitivity behavior for the two states even if their remanence values were equal.

In view of those questions, materials differing substantially from the previously discussed optimum of 60 percent NiFe were studied. Samples included were:

- | | |
|---|----------|
| 1. Carpenter High-permeability "49-FM" (rod) | 49% NiFe |
| 2. Superior Tube 52 Alloy ("Weldrawn" tube) | 50% NiFe |
| 3. Superior Tube "A" Nickel (Seamless tube) | 99.6% Ni |
| 4. Superior Tube Nickel 204 ("Weldrawn" tube) | 4% CoNi |

5. H. K. Porter "A" Nickel (Rod)	99% Ni (min.)
6. H. K. Porter Incoloy 805 (Rod)	36-54.5-7.5% NiFeCr
7. Wilbur B. Driver "Balco" (Rod)	70% NiFe

Incoloy 805 has a resistivity approximately ten times than of Ni and twice that of 49 percent NiFe so its lower losses should be an advantage in high-frequency operation. 4 percent CoNi, developed ⁸ initially for magnetostrictive transducers, recently became commercially available in thin-wall tubing.

The above samples were tested in the following three tempers:

1. As received; all samples cold-drawn, except 70 percent NiFe which had an intermediate temper.
2. Annealed in dry hydrogen one hour at 1400°F.
3. Annealed in dry hydrogen 4 hours at 2100°F and cooled at a rate of less 100°F/hr.

4.2 SIGNAL-TO-NOISE AND OUTPUT CRITERIA

Remanent strain sensitivity, as explained above, is the material property of primary initial concern in magnetoacoustic storage. In measurements reported subsequently, strain sensitivity is indicated by the change of induction ΔB resulting from a given $\Delta \sigma$. In particular

ΔB_{RH} = change in remanence for a given $\Delta \sigma$ when the initial remanence is produced by H alone.

$\Delta B_{RH\sigma}$ = change in remanence for the given $\Delta \sigma$ when the initial remanence is produced by H in the presence of σ .

The relation of these parameters to the S/N and output level for the magnetoacoustic memory was derived as follows, assuming the medium is stress biased as discussed in Section 4.4.2. For a perfectly uniform storage medium,

the peak output signal is

$e_s = K(\Delta B_{RH} - \Delta B_{RH\sigma})$, where K is a constant which includes the effects of the time derivative and pulse slope as determined by electrical and mechanical time constants.

Let u be a factor representing the uniformity of the medium such that $u_0 = 1$ corresponds to the average sensitivity, and the maximum and minimum limits are u_2 and u_1 , respectively. The minimum signal level and maximum noise level, respectively, are then

$$e_{s \text{ min}} = K(u_1 \Delta B_{RH} - u_2 \Delta B_{RH\sigma})$$

$$e_{n \text{ max}} = K(u_2 \Delta B_{RH\sigma} - u_1 \Delta B_{RH\sigma})$$

S/N is

$$\frac{e_{s \text{ min}}}{e_{n \text{ max}}} = \frac{u_1 \Delta B_{RH} - u_2 \Delta B_{RH\sigma}}{\Delta B_{RH} (u_2 - u_1)} = \frac{1}{u_2 - u_1} \left(\frac{u_1 \Delta B_{RH}}{\Delta B_{RH\sigma}} - u_2 \right)$$

Setting $u_2 \cong 1/u_1$, $\frac{e_{s \text{ min}}}{e_{n \text{ max}}} = \frac{u_1^2 R - 1}{1 - u_1^2}$, where $R = \frac{\Delta B_{RH}}{\Delta B_{RH\sigma}}$

Representative values of R vs u required to obtain 10 db S/N are then:

u_1	R
0.99	1.09
0.97	1.3
0.90	2.0
0.80	3.3
0.70	5.3

Hence, if u varies ± 10 percent, e.g., in accordance with the commercial tolerance on the wall thickness of thin tubing, 10 db S/N could be obtained with

$$\frac{\Delta B_{RH}}{\Delta B_{RH\sigma}} = R = 2$$

Signal output is also a function of R:

$$e_s = K(\Delta B_{RH} - \Delta B_{RH\sigma}) = K(\Delta B_{RH} - \Delta B_{RH\sigma}) \frac{\Delta B_{RH}}{\Delta B_{RH}} = K(1-1/R)\Delta B_{RH}$$

$$\lim_{R \rightarrow \infty} e_s = K\Delta B_{RH}$$

$$\lim_{R \rightarrow 1} e_s = 0$$

For $R = 2$, $e_s = 0.5 K \Delta B_{RH}$, or half its maximum value for $R = \infty$. By comparison, operation at low values such as $R = 1.1$, e.g., would reduce the output to 0.1 of its maximum value, and a S/N of 10 db would require a uniformity of $\pm 1\%$.

Hence, a primary purpose of materials studies is to determine how the ratio, $R = \Delta B_{RH}/\Delta B_{RH\sigma}$ varies with operating levels H and σ , and with material composition and anneal.

4.3 SIGNAL STABILITY

Two forms of stability were investigated in initial studies. The first involves evaluation of the decay in signal level which results from repetitive readout. For a particular set of conditions, Bozorth⁹ has shown substantial decay, in the induction of 68 Permalloy when stressed repeatedly. Negligible decay, however, is required to permit non-destructive readout in magnetoacoustic storage. In particular, it was to be determined whether hard-drawn materials in general provide better stability than annealed materials.

A second form of stability involves the effect of a reversed polarizing field during writein for Mode (2), as discussed in Section 2.0. For this mode, conditions are desired such that a reversal of H will cause negligible change in a

previously recorded bit at addresses where σ is absent, but will produce a complete reversal of remanence at the address of a coincident stress pulse. Hysteresis loops under longitudinal conditions as reported for 68 Permalloy by Bozorth¹⁰, e.g., show a large reduction in coercive force when the material is subjected to stress, as well as relatively square loops for the stressed and unstressed conditions. Consequently, it was expected that materials and operating levels could be established which would cause negligible change in remanence with stress absent but complete reversal of remanence with stress present.

4.4 INITIAL MATERIALS STUDY

4.4.1 PROCEDURES

The point-by-point data required for systematic analysis of the basic B-H- σ cycle were obtained by fluxmeter measurement. Suitably large readings required relatively heavy material samples in the form of tubes 2 inches long by 0.125" OD with 20-mil wall thickness. Non-magnetic flanges were epoxied to the ends of samples so they could be slipped into grooves in specially designed stress apparatus. The samples were provided with a pair of B and H windings in toroidal form to permit measurement of transverse properties. Figures 4.1 and 4.2 show a modified sample, epoxying fixture, and stress apparatus used for the later measurements reported in Section 4.5.2. The flanges used in initial measurements were in the form of 3/4 inch by 1-11/16 inches rectangular plates, which were epoxied to the tube sample in an accurately milled fixture to assure perpendicularity. The purpose of the large plates used initially was to minimize any tendency of the sample to buckle under compressive stress and to aid in achieving alignment between sample and the driving blocks of the stress rig.

Three sets of data for each sample were obtained as follows:

1. Magnetization curves at appropriate stresses
2. Transverse strain sensitivity under three conditions:

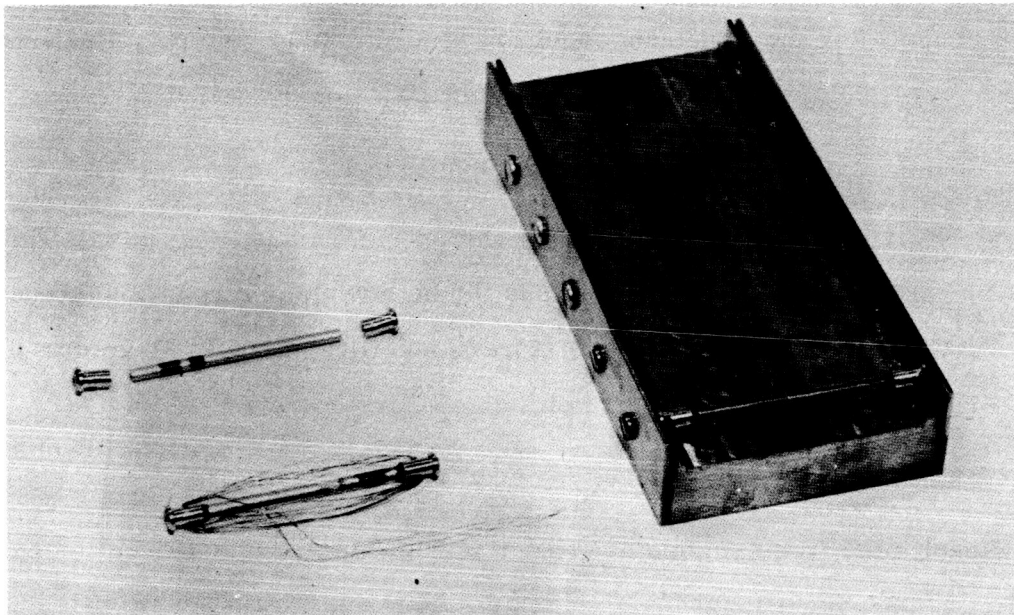


Figure 4.1. Material Sample Assembly and Bonding Fixture.

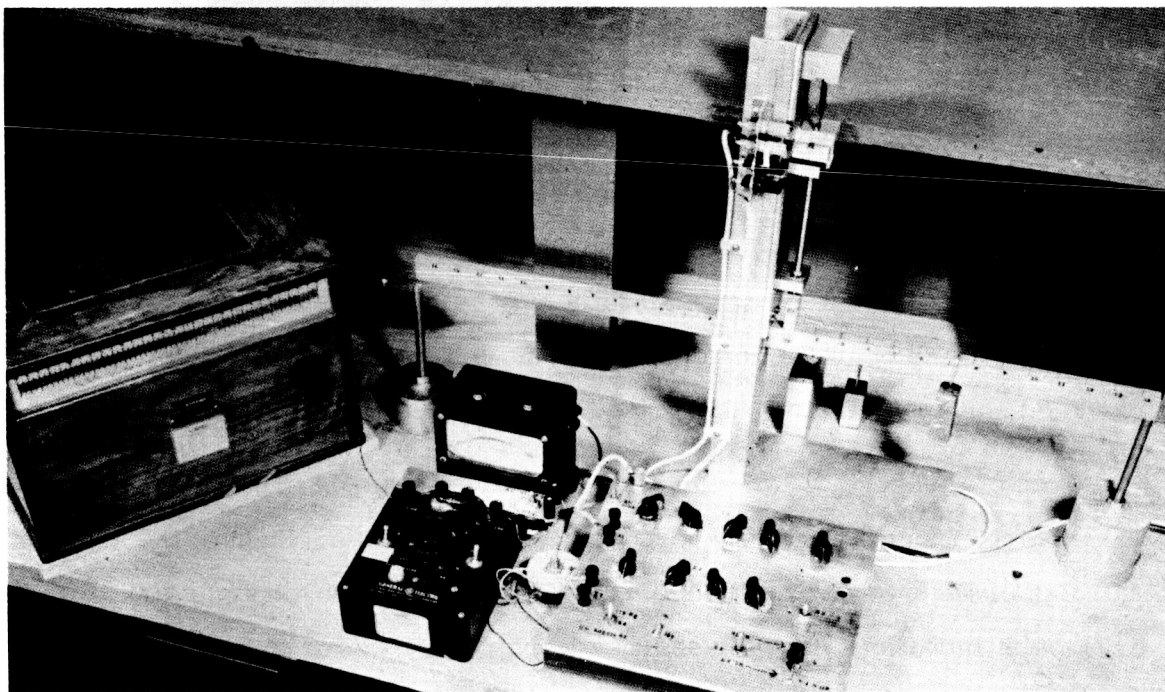


Figure 4.2. Test Apparatus.

- (a) For the remanent condition resulting from a prior application of polarizing field in the presence of stress
 - (b) For the remanent condition resulting from prior application of a polarizing field to the unstressed sample
 - (c) With external polarization applied
3. Write-read cycles simulating the magnetoacoustic process. These show the actual $B-H-\sigma$ history for both write and read; include several readout cycles to indicate storage stability; and, finally, show the effect of a reverse polarizing field.

4.4.2 MAGNETIZATION CURVES

Results for five samples are shown in Figures 4.3 through 4.7. The curves serve as an orientational indication of comparative strain sensitivities and magnetizing field requirements. Stresses required for a given change of induction average an order of magnitude higher for the hard-drawn samples than for the annealed samples. Use of hard-drawn materials, therefore, would require relatively elaborate transducers and/or acoustical transformers to accomplish magnetoacoustic storage. However, acoustical losses in hard materials are lower ¹¹ and they may be preferred for relatively long, high-capacity lines. Moreover, general experience with magnetic materials in conventional applications suggests that the harder materials may be more stable during repeated readout and may operate more effectively at remanence. Consequently, both hard and soft materials were carried through the complete series of tests.

Both of the hard-drawn samples of Figures 4.6 and 4.7 show the expected increase in induction for transverse (axial) compression. Each of the annealed samples of Figures 4-3 through 4.5, however, shows unexpectedly small increases of induction. In all cases data were rerun at zero stress after the high-stress runs to be certain that the elastic limit had not been exceeded.

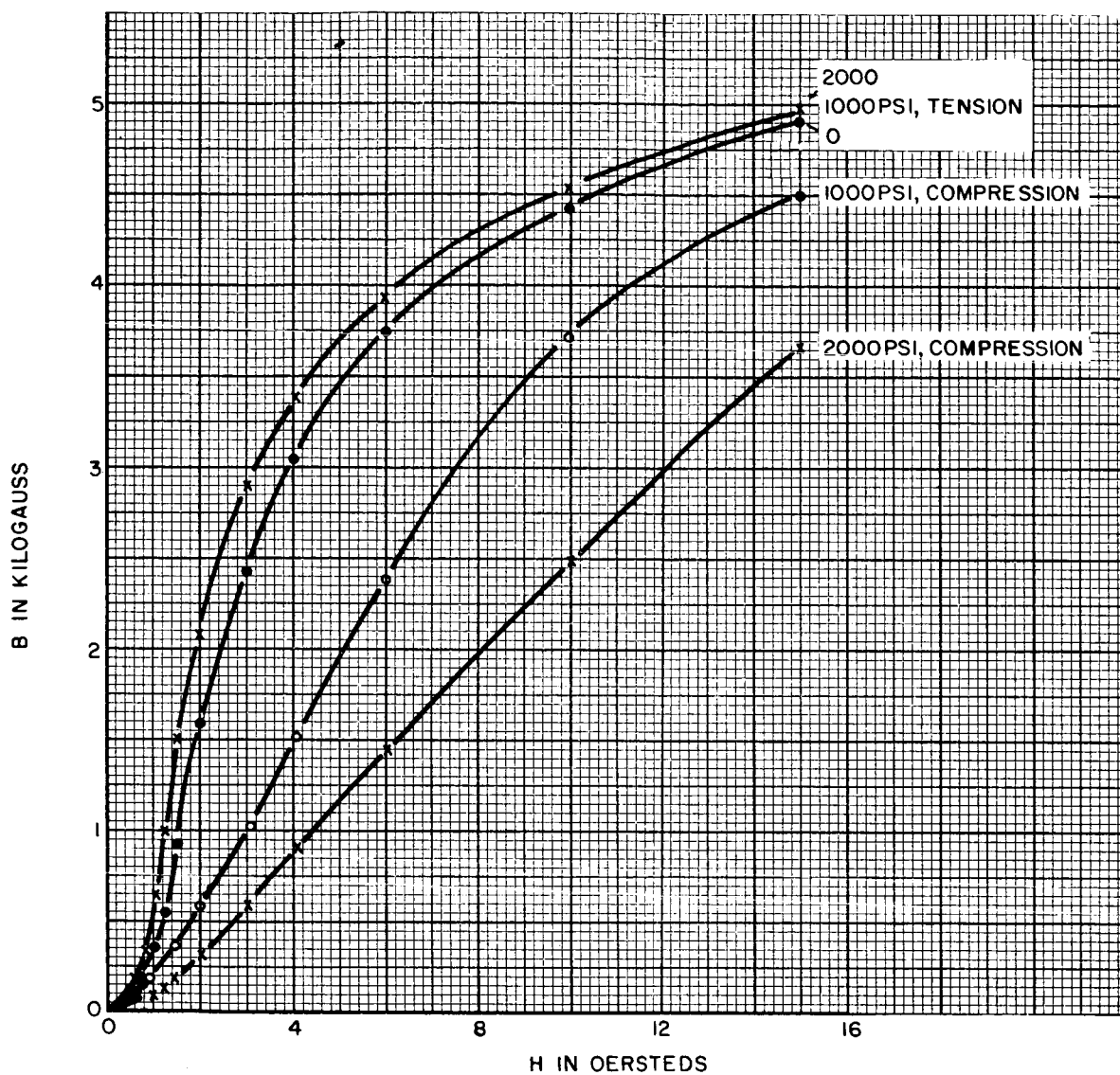


Figure 4.3. Magnetization Curves for Annealed Nickel.

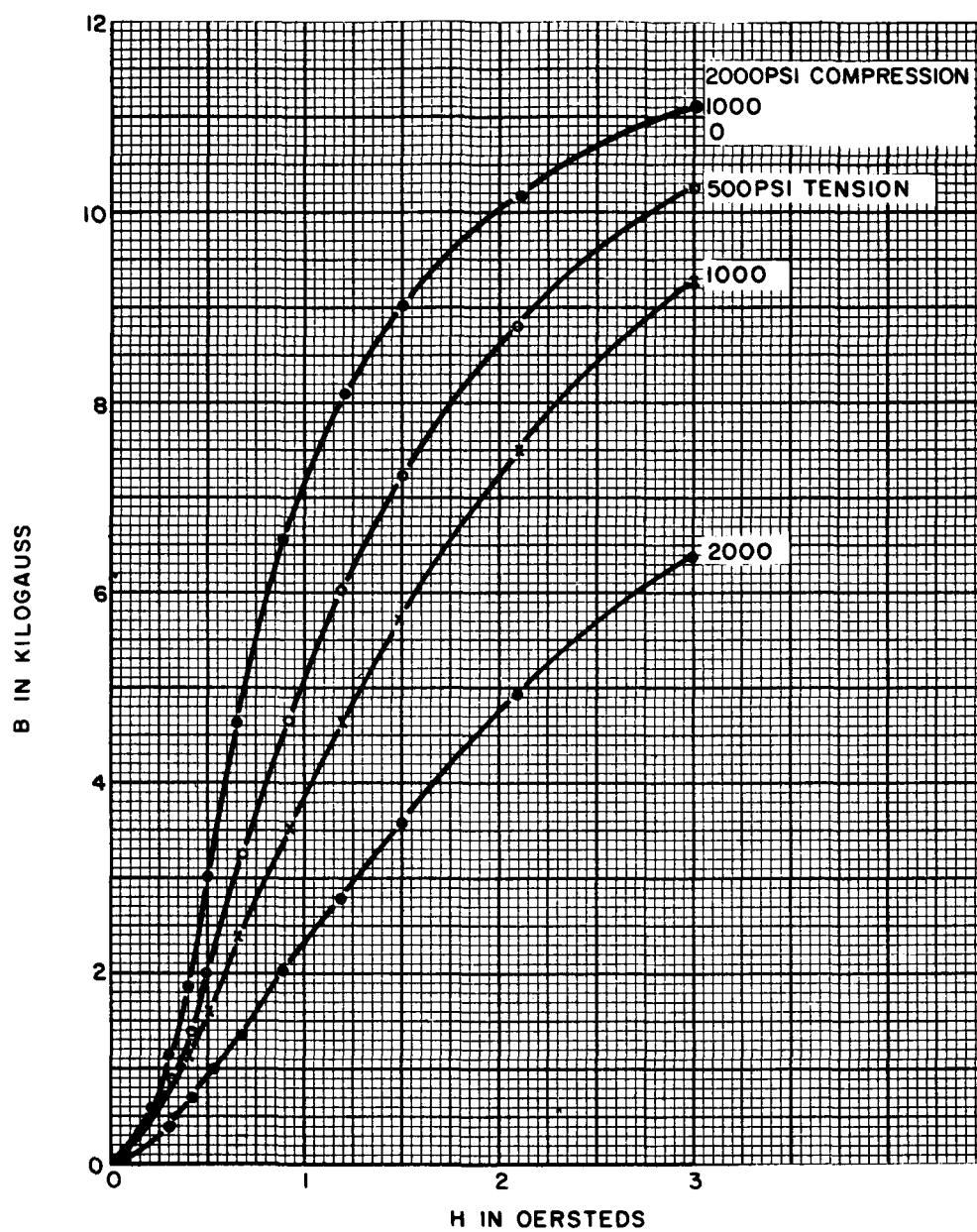


Figure 4.4. Magnetization Curves for Annealed NiFe.

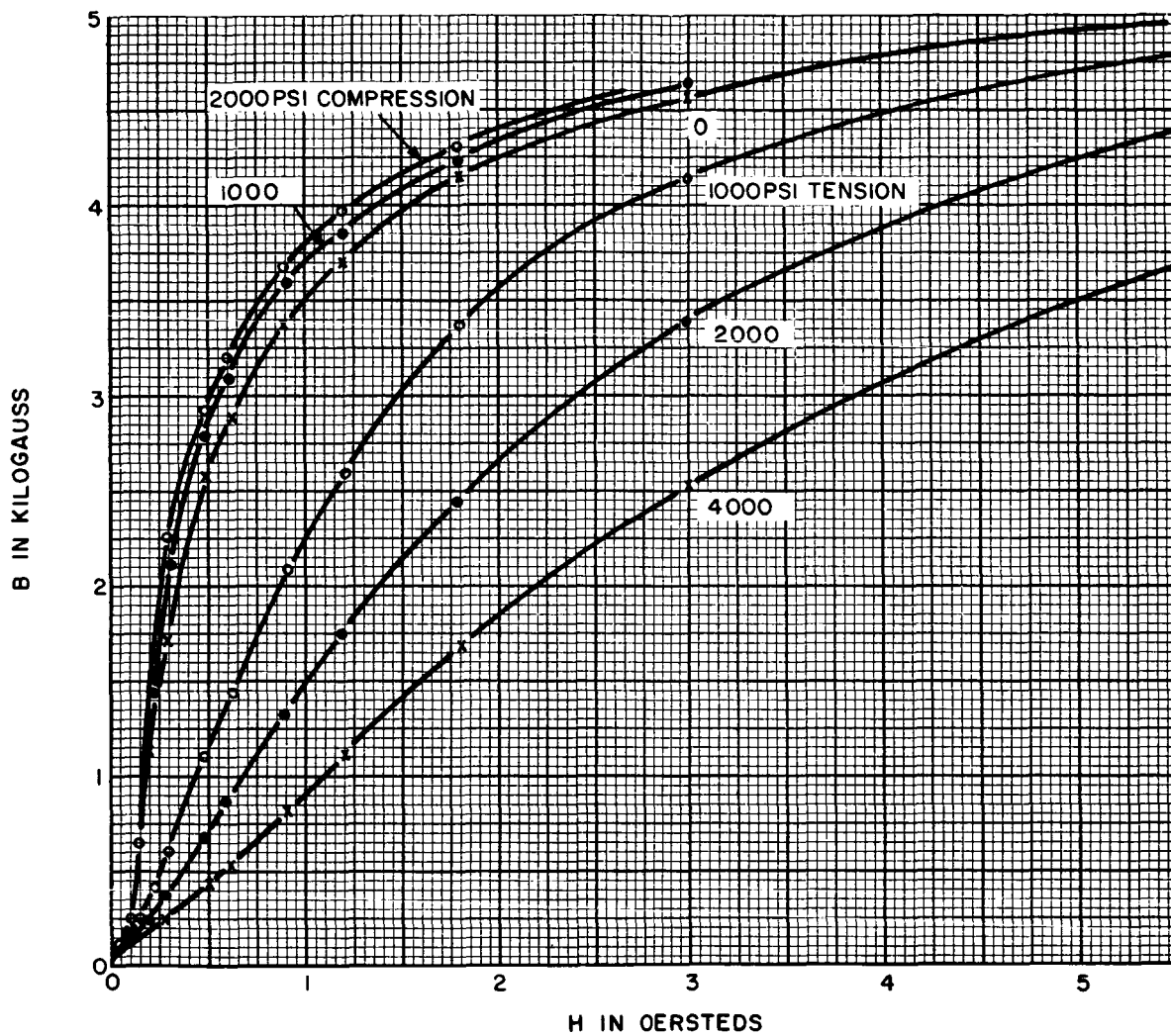


Figure 4.5. Magnetization Curves for Annealed NiFeCr.

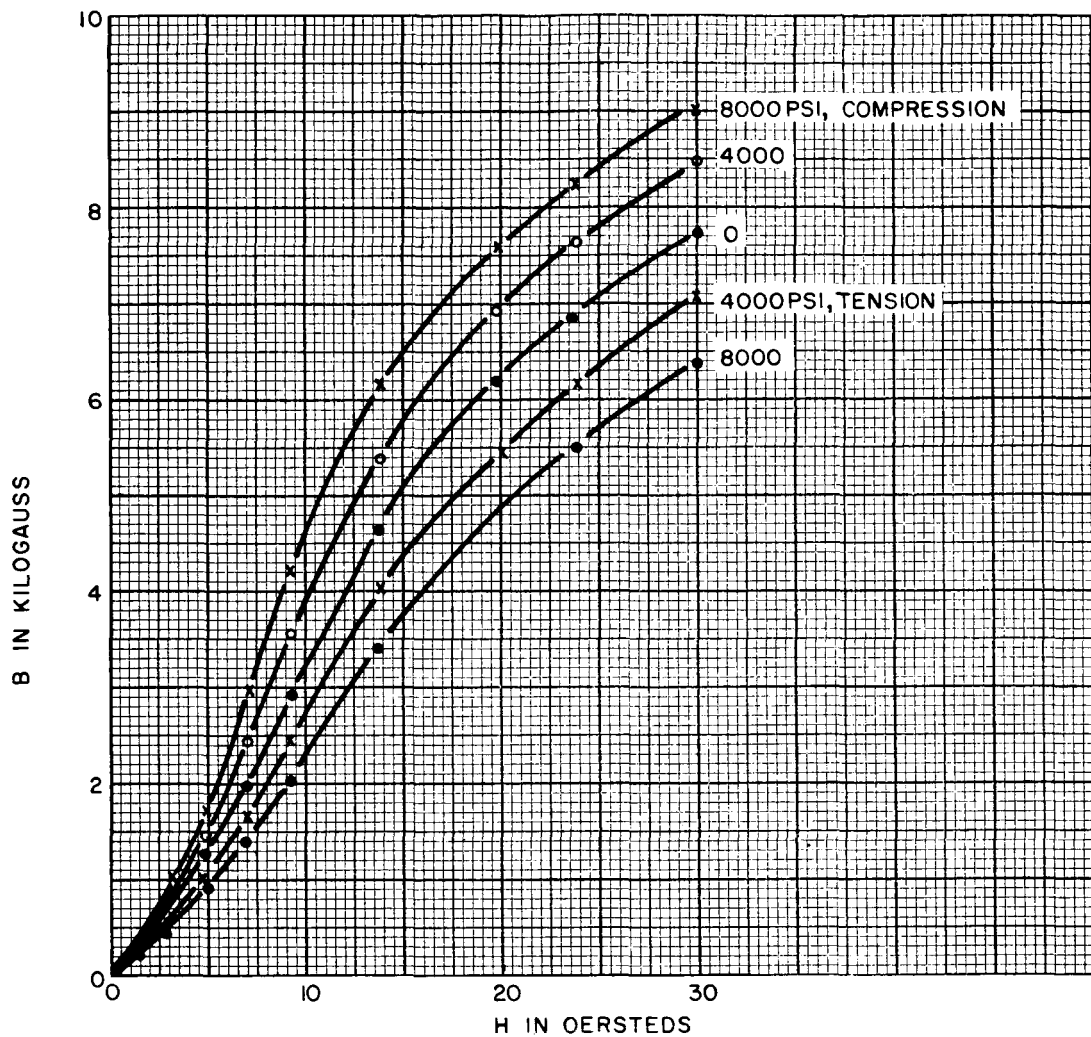


Figure 4.6. Magnetization Curves for Hard-Drawn NiFe.

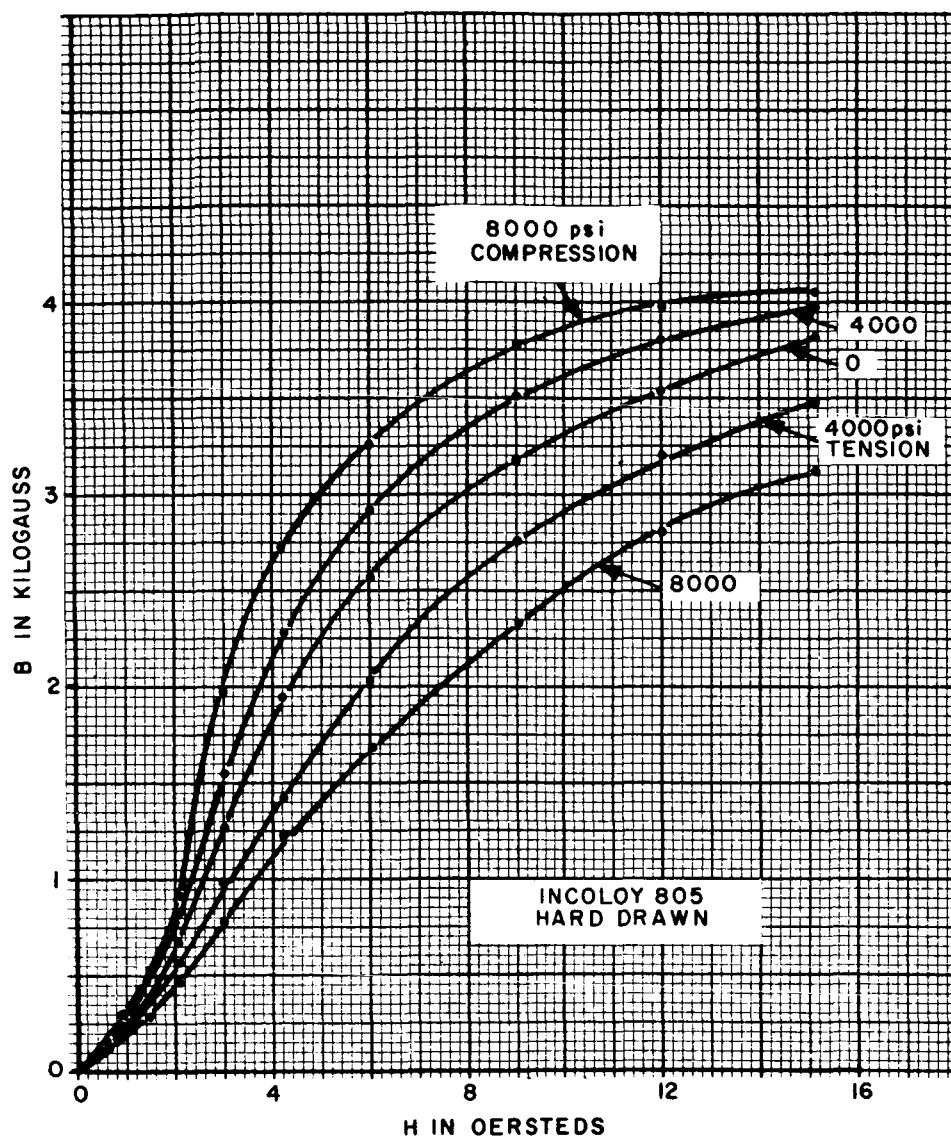


Figure 4.7. Magnetization Curves for Hard-Drawn NiFeCr.

This result is partly explained by the fact that an anomalous bending moment, which places half of the sample cross section in tension and half in compression, tends to reduce circumferential induction. Bozorth¹² shows that the change of induction for a fixed value of H is a linear function of σ for small $\Delta\sigma$ of either sign, i.e.,

$$B = B_0 \pm a\sigma$$

The circumferential reluctance for a sample section, half in tension and half in compression, is then

$$\begin{aligned} R_c + R_t &= K \left(\frac{1}{B_0 + a\sigma} + \frac{1}{B_0 - a\sigma} \right) \\ &= K \left[(B_0^{-1} - a\sigma + B_0^{-3} a^3 \sigma^3 - \dots) + (B_0^{-1} + a\sigma + B_0^{-3} a^3 \sigma^3 + \dots) \right] \\ &= \frac{2K}{B_0} \left[1 + \left(\frac{a\sigma}{B_0} \right)^2 + \dots \right], \text{ which converges for } a\sigma < B_0 \end{aligned}$$

When $\sigma = 0$,

$$R_{c0} + R_{t0} = 2K/B_0$$

Consequently, a bending moment tends to increase circumferential reluctance. Annealed materials having low internal strains are more sensitive to the effect of external strain than cold-drawn materials, and require very accurate alignment to avoid a decrease of induction relative to the value at zero stress. Because of the low strain sensitivity observed at the higher induction levels, as well as the more critical material-handling and support requirements involved, operation with strain bias was investigated. Materials of positive magnetostriction, which are preferred because of their relatively high strain sensitivity, require a tensile bias for this purpose, and this could be accomplished by practicable tensioning means in the thin lines required for actual memories. The following data, therefore, were obtained under conditions such that the sample is stress

biased to a low value of induction for zero-signal simulation; the stress bias is then removed in the presence of a polarizing field to simulate writein.

4.4.3 STRAIN SENSITIVITY

Figures 4.8 through 4.12 show representative strain-sensitivity data for five material samples under externally polarized conditions as well as remanent conditions. Each figure shows change of induction, for a given $\Delta\sigma$, as a function of maximum applied field intensity.

Referring to Figure 4.3 for annealed nickel, the ΔB_H curve represents the externally polarized condition. Each point was obtained by advancing the magnetizing field to a desired value, cycling $\pm H$ several times, then applying and removing the specified stress three times during which the change of induction was observed. The final change of induction is plotted as the ordinate. Data for ΔB_{RH} were obtained by the same process except that H was removed before applying stress so that the change in remanent induction was measured. To obtain $\Delta B_{RH\sigma}$, the specified stress was applied while the material was cycled $\pm H$; H was then removed and $\Delta B_{RH\sigma}$ thus represents the change of induction for readout of the zero signal level since the stress served to bias the storage element to a low value of induction. ΔB_{RH} shows the change of induction for readout of a signal represented by removal of stress; in an actual storage system, this would be accomplished by propagating a compressive stress pulse equal in magnitude to that of the tensile stress bias for a positive material, or vice versa for negative materials.

These procedures were modified for the hard-drawn samples of Figures 4.11 and 4.12. Since compressive stress did provide increased induction in the hard-drawn samples, compression could be added to the zero-stress-biased sample to simulate the writein operation. Consequently, data for both tensile and compressive stress are shown in Figure 4.11 for hard-drawn NiFe, and only the zero-biased simulation is shown in Figure 4.12 for hard-drawn NiFeCr.

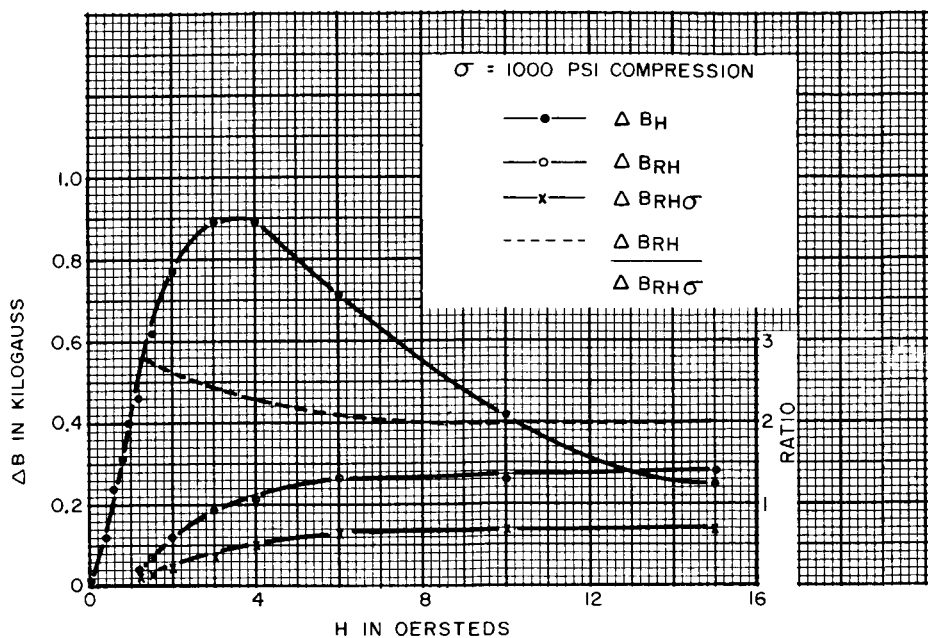


Figure 4.8. Strain Sensitivity for Annealed Nickel.

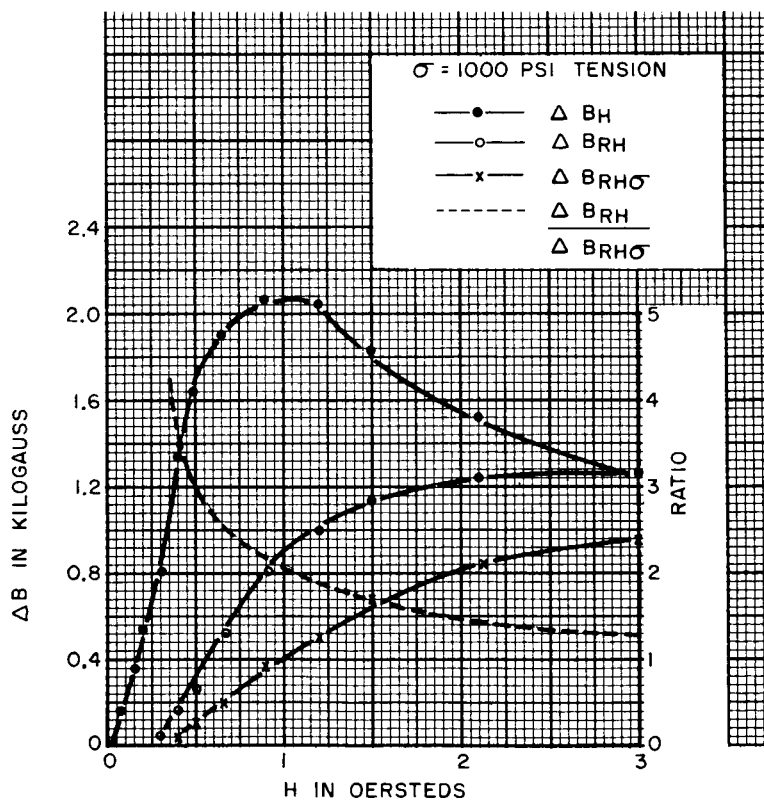


Figure 4.9. Strain Sensitivity for Annealed NiFe.

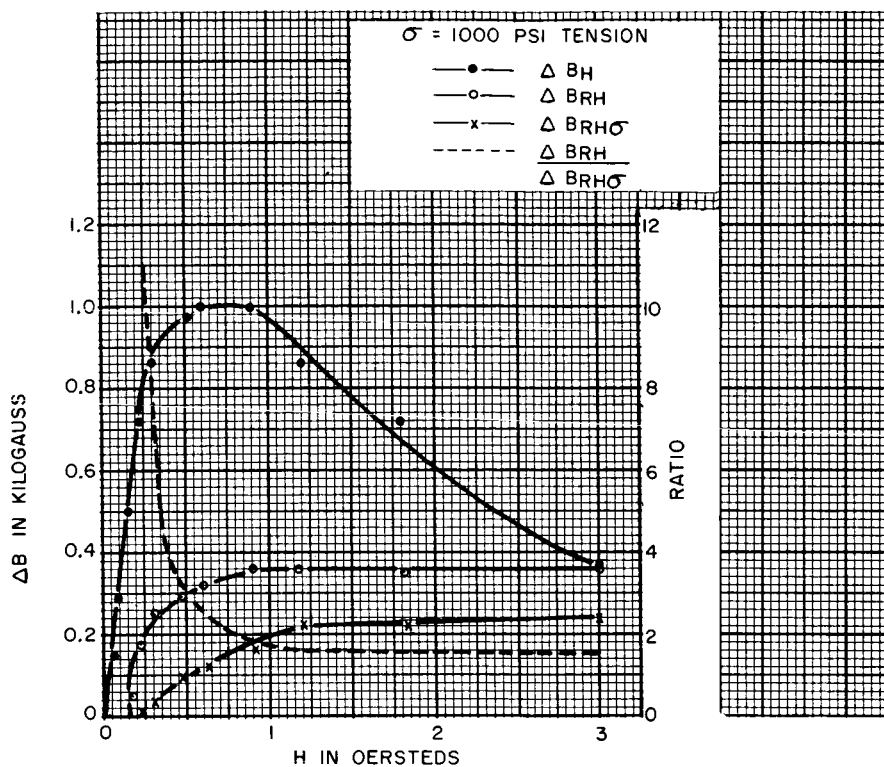


Figure 4.10. Strain Sensitivity for Annealed NiFeCr.

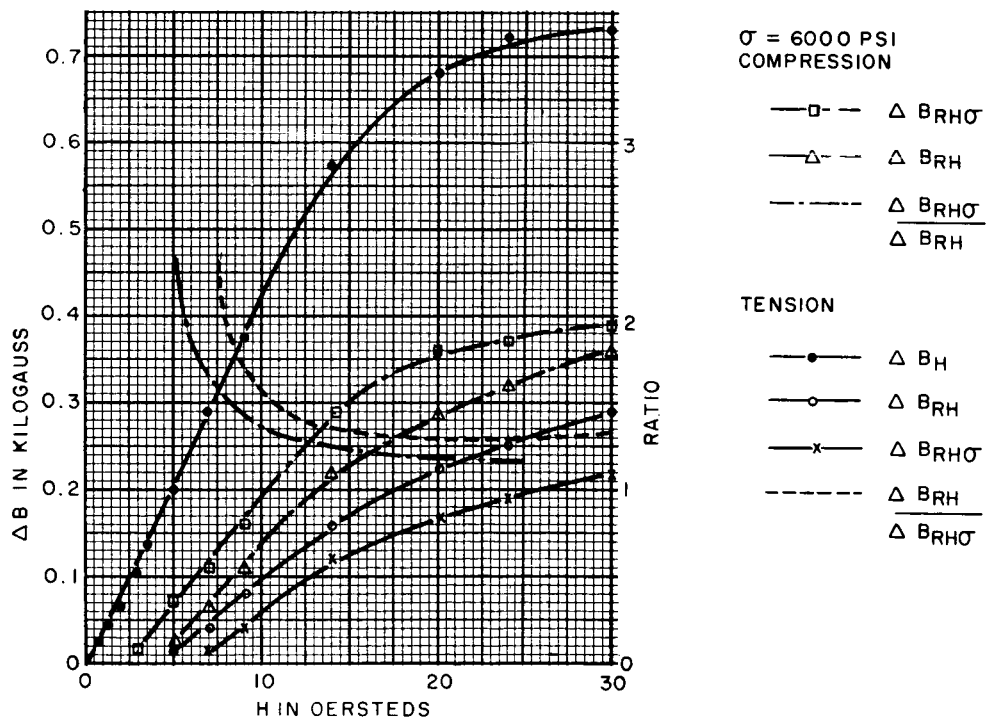


Figure 4.11. Strain Sensitivity for Hard-drawn NiFe.

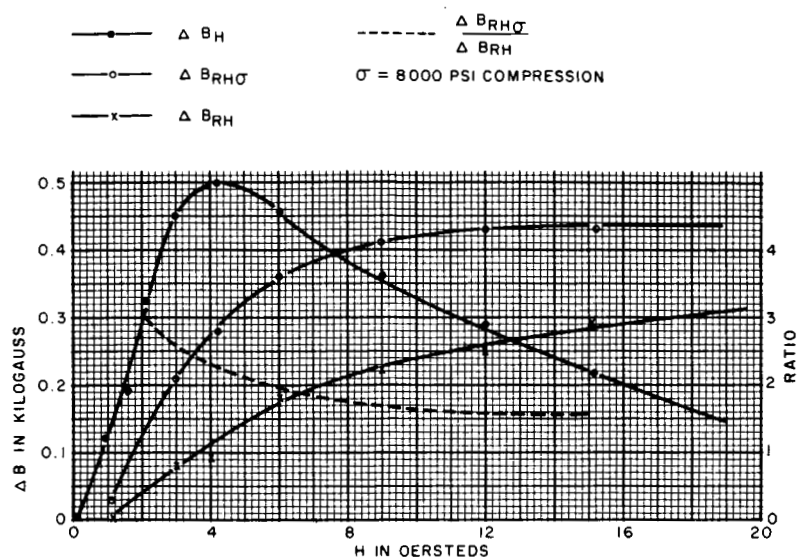


Figure 4.12. Strain Sensitivity for Hard-drawn NiFeCr.

The dashed line shown in the figures is the ratio of $\Delta B_{RH}/\Delta B_{RH\sigma}$, or $\Delta B_{RH\sigma}/\Delta B_{RH}$ in the case of hard-drawn samples where the zero-biased condition is simulated. Determination of this characteristic was one of the primary objectives of the study because, as explained in Section 4.2, both S/N and output level are expected to improve as the ratio is increased. Each of the samples shows a rapid rise in the ratio as H approaches zero.

Since the magnetization curves for hard-drawn samples show relatively uniform changes in induction for compressive as well as tensile stresses, operation could be tested under conditions corresponding to zero biasing stress. Consequently, for Figure 4.11, writein was simulated by applying a compressive stress in the presence of a polarizing field as originally proposed, as well as by removing a tensile bias. The data show that, for a given strain sensitivity, the ratio R is approximately the same with either set of operating conditions.

The annealed samples of 49 percent NiFe and NiFeCr have the most interesting characteristics for magnetoacoustic storage. The remanent strain sensitivity of the NiFe provides a change of 1200 gauss for high recording levels, whereas that for NiFeCr is less than one-third as large. However, comparison for lower polarizing fields, such that the ratio $\Delta B_{RH}/\Delta B_{RH\sigma} = 4$, shows ΔB_{RH} for NiFeCr

to be 1.7 times that for NiFe, and ΔB_{RH} is still a substantial 200 gauss when the ratio has reached 10 for the NiFeCr alloy. These data coupled with the criteria of Section 4.2 indicate that it should be possible to achieve good S/N from Mode (1) operation using a stress-biased storage medium. The ratio $R = 10$, e.g., should yield better than 30 db S/N if the medium is uniform within ± 10 percent. The data correspond to a practical value of 1000 psi for the applied stress.

4.4.4 WRITE-READ CYCLE

Typical B-H- σ histories for the five samples, as shown in Figures 4.13 through 4.17, were obtained in order to clarify understanding of the actual storage and readout processes. In all cases except hard-drawn NiFeCr, two values of H_{max} were chosen from the strain sensitivity data. In general, the larger value of H_{max} corresponds to a point near the knee of the magnetization curve and a value of R on the horizontal portion of the ratio curve. The lower value of H_{max} corresponds to a point near the instep of the magnetization curve and a value of R on the steeply rising portion of the ratio curve.

Referring to the detailed description of sequences shown in Figure 4.13 for annealed Ni, the sample was first cycled $\pm H_{max}$ with stress bias removed, thus simulating a storage element which had been repeatedly rerecorded in the past, and was left finally with a positive induction when H was returned to zero. The stress bias was then applied, corresponding to the quiescent state after passage of a stress pulse, and the remanence dropped as indicated. Next, the sample was subjected to a series of stress cycles, corresponding to readout, and the resulting variations of remanence at $H = 0$ were plotted as a sequence to the left of the hysteresis loop; the abscissa for the insets is the step sequence consisting of repeated applications and removals of stress.

Negative H_{max} was then applied and removed in the presence of the stress bias. This simulates the erasing effect on a given cell, previously recorded with a ONE, when polarizing field is applied to the whole line to record a ZERO at some other site along the line. The readout stress was again applied repeatedly,

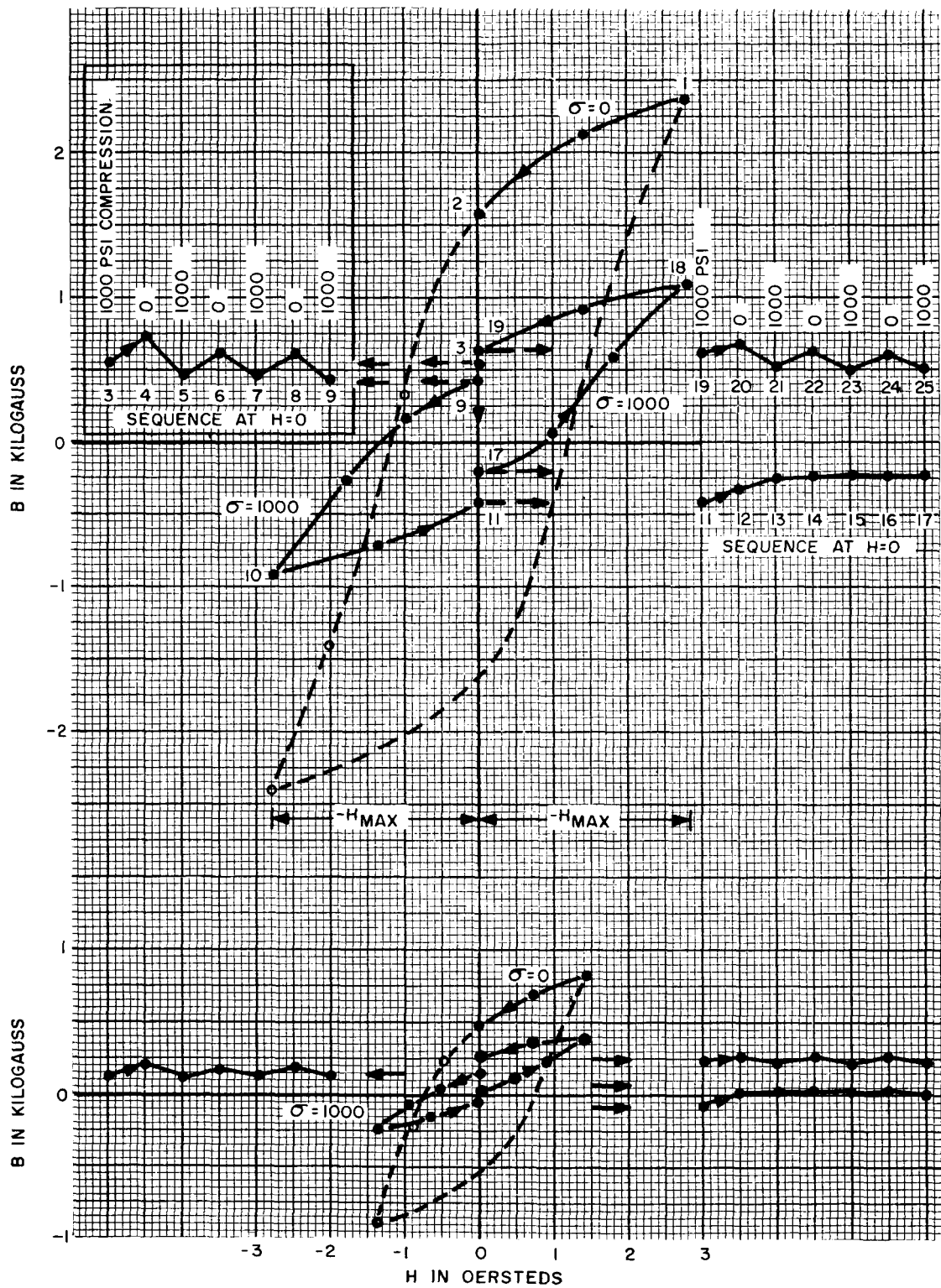


Figure 4.13. Write-Read Cycle for Annealed Nickel.

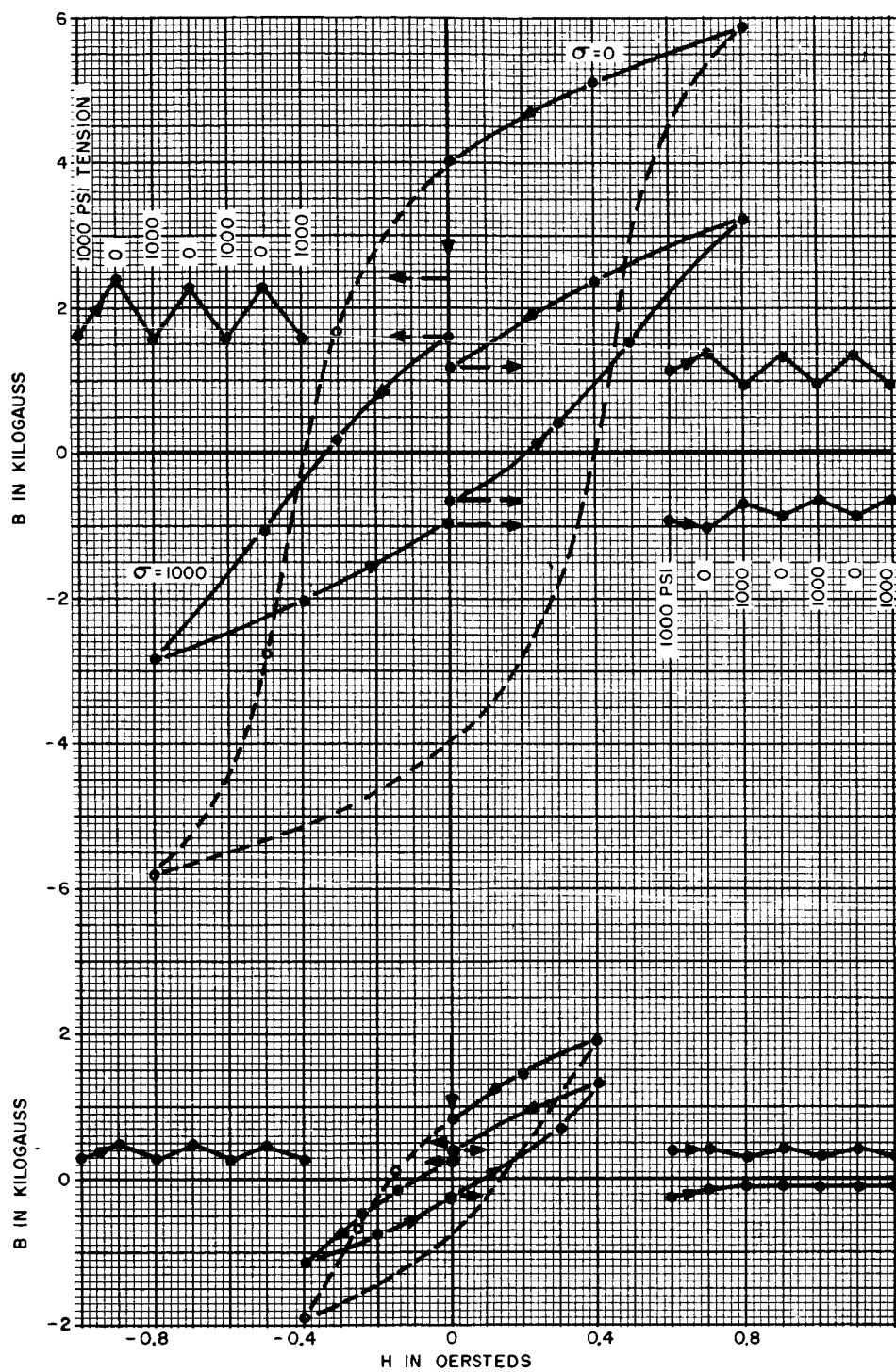


Figure 4.14. Write-Read Cycle for Annealed NiFe.

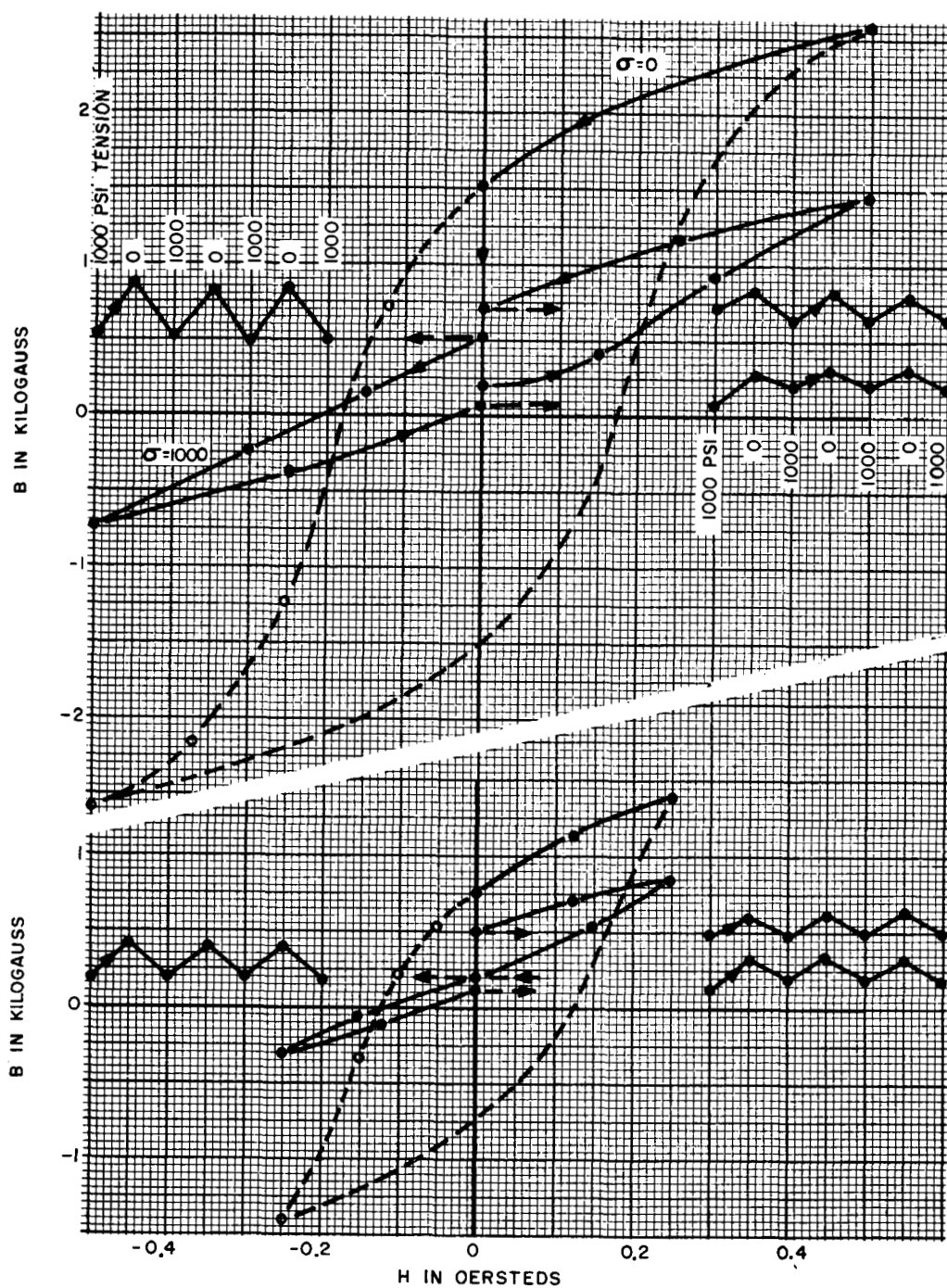


Figure 4.15. Write-Read Cycle for Annealed NiFeCr.

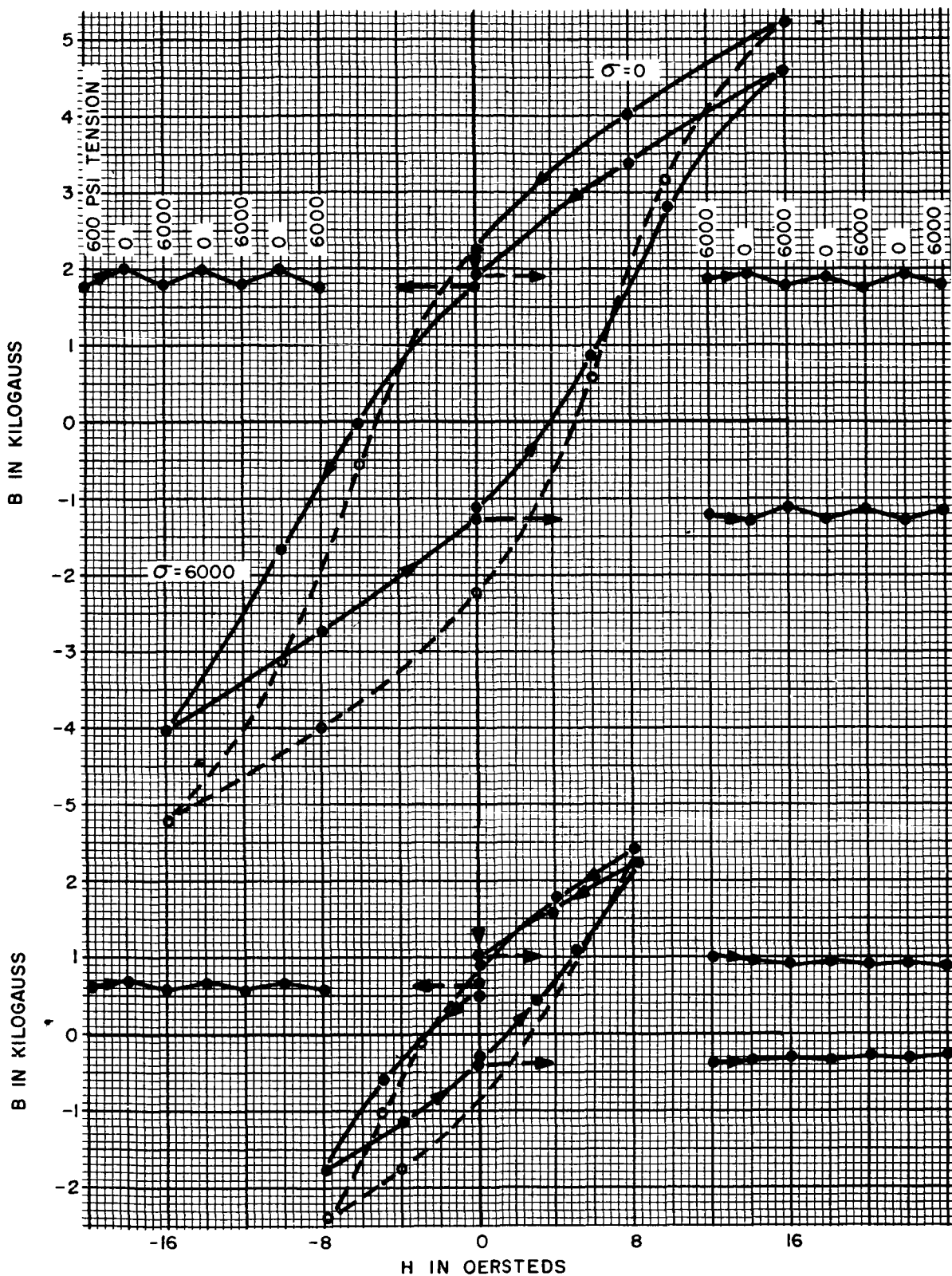


Figure 4.16. Write-Read Cycle for Hard-Drawn NiFe.

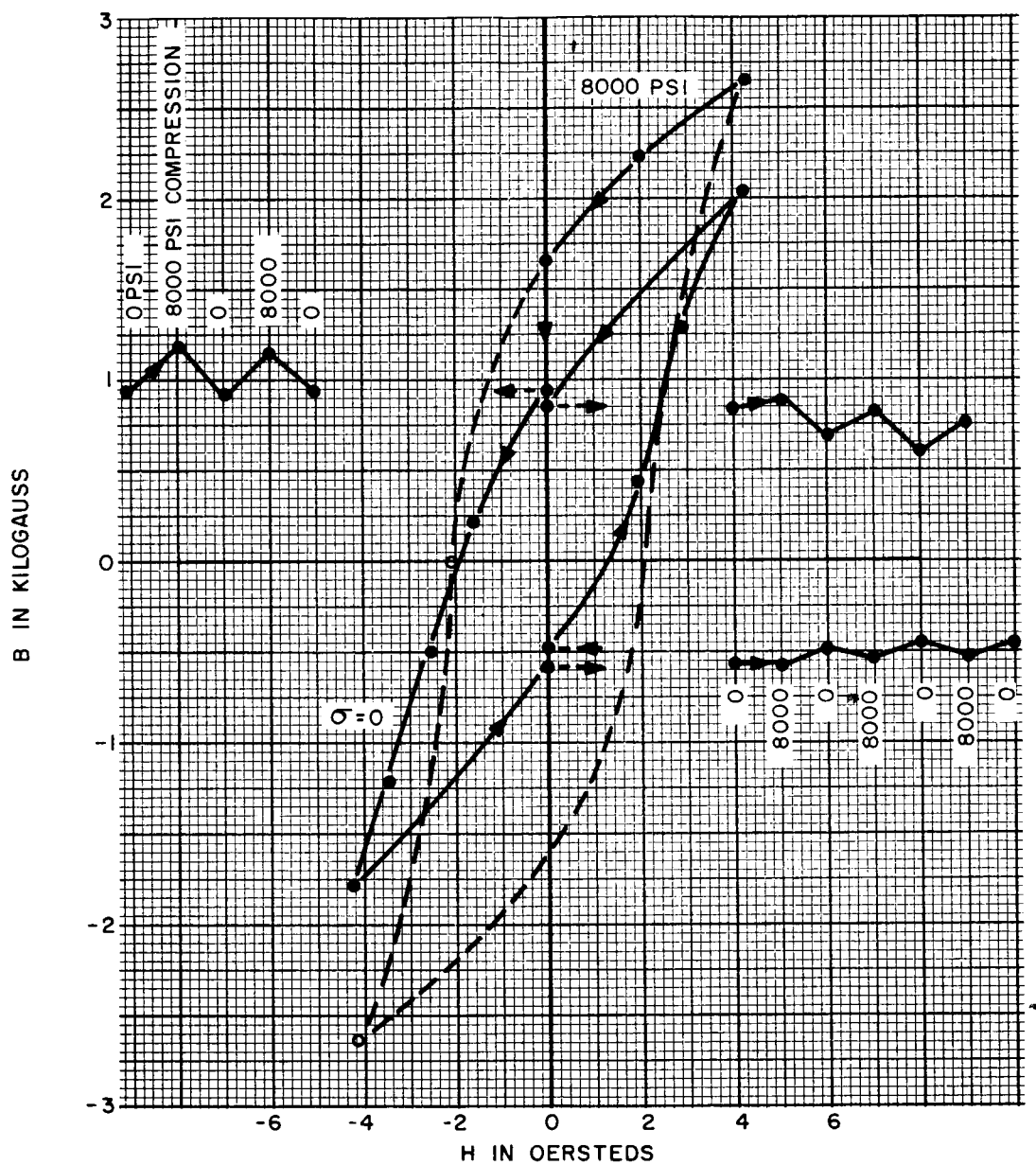


Figure 4.17. Write-Read Cycle for Hard-Drawn NiFeCr.

and the result is plotted as the lower right-hand sequence. At this point the 49 per-cent NiFe of Figure 4.14, e. g. , shows complete erasure of the original signal for the lower value of H_{\max} (in the lower figure) and actual reversal for the larger value of H_{\max} (in the upper figure). That is, removal of stress bias originally caused an increase of induction, but after application of the reverse field, removal of stress bias produced a decrease of induction. The third stress sequence plotted at the upper right shows readout after applying positive H_{\max} in the presence of the biasing stress. Ideally, each of these sequences should be identical.

The one sample approaching the desired result is the annealed NiFeCr alloy of Figure 4.15. The stability for the lower value of H_{\max} is the best obtained and, in addition, it corresponds to a value of $R = 10$ on the strain sensitivity curves of Figure 4.10. Improved stability at the lower values of H_{\max} occurs also with the other samples, but in those cases erasure still occurs even though reversal is avoided.

The write-read data show that generally there is a relatively small change in output during repeated readout, so non-destructive readout can be obtained. The downward drift in average value will not be of concern in actual systems with appropriate coupling time-constants, and the incremental change stabilizes after the first few cycles, during which it is sufficiently small to be tolerated in digital systems.

The operation emphasized in the write-read cycles corresponds to the preferred Mode (2) as discussed in Section 2.0. Because ZEROS and ONES in this case are to be stored as plus and minus values of induction, rather than plus and zero, the S/N and output-level criteria discussed in the preceding section do not apply. Conversely, the requirement that a recorded element tolerate reverse H without appreciable erasure does not apply to operation under Mode (1), and the data of the previous section relate primarily to Mode (1) operation. Mode (1) operation is accomplished with each of the materials discussed but best S/N and output levels would be obtained from the annealed NiFeCr alloy. That sample

also comes closest to meeting the Mode (2) requirements. The NiFeCr alloy has not been evaluated dynamically because it is not commercially available in thin-wall tubing. Further understanding of additional considerations discussed subsequently appears desirable before special work can be justified for the development of techniques for drawing new alloys into thin-wall tubing.

4.5 ADVANCED MATERIALS ANALYSIS

4.5.1 TRANSVERSE STRAIN SENSITIVITY

The poor transverse strain sensitivity observed for annealed positive materials when compressed axially, or negative materials in axial tension, imposes a serious basic limitation on the magnetoacoustic storage process, as noted in Section 4.1. Explanation of the cause and a solution to the problem should offer major opportunities for improvements in memory efficiency and S/N, which may then be compromised to provide further gains in resolution, transducer and constructional simplicity, and relaxation of electrical and mechanical tolerances.

4.5.1.1 TESTS

To permit a more rapid study of changes in gross material properties with stress, AC B-H loop tracer techniques were substituted for the fluxmeter measurements previously employed. Changes in hysteresis loops and magnetization curves could then be observed immediately as adjustments were made in the mechanical alignment of test samples. The need for a more accurate stress rig was confirmed, and design and construction of modified apparatus for the subsequent detailed B-H- σ studies discussed in Section 4.5.2 was undertaken. Even with optimum sample alignment in the original apparatus, however, it was found that the transverse strain sensitivity of positive annealed materials for axial compression was one to two orders of magnitude poorer than expected. Each of the first six samples listed in Section 4.1 was tested. The results shown in Figure 4.18 for 49 percent NiFe are representative of the best obtained. The magnetization curves were obtained under cyclic conditions using Z-axis

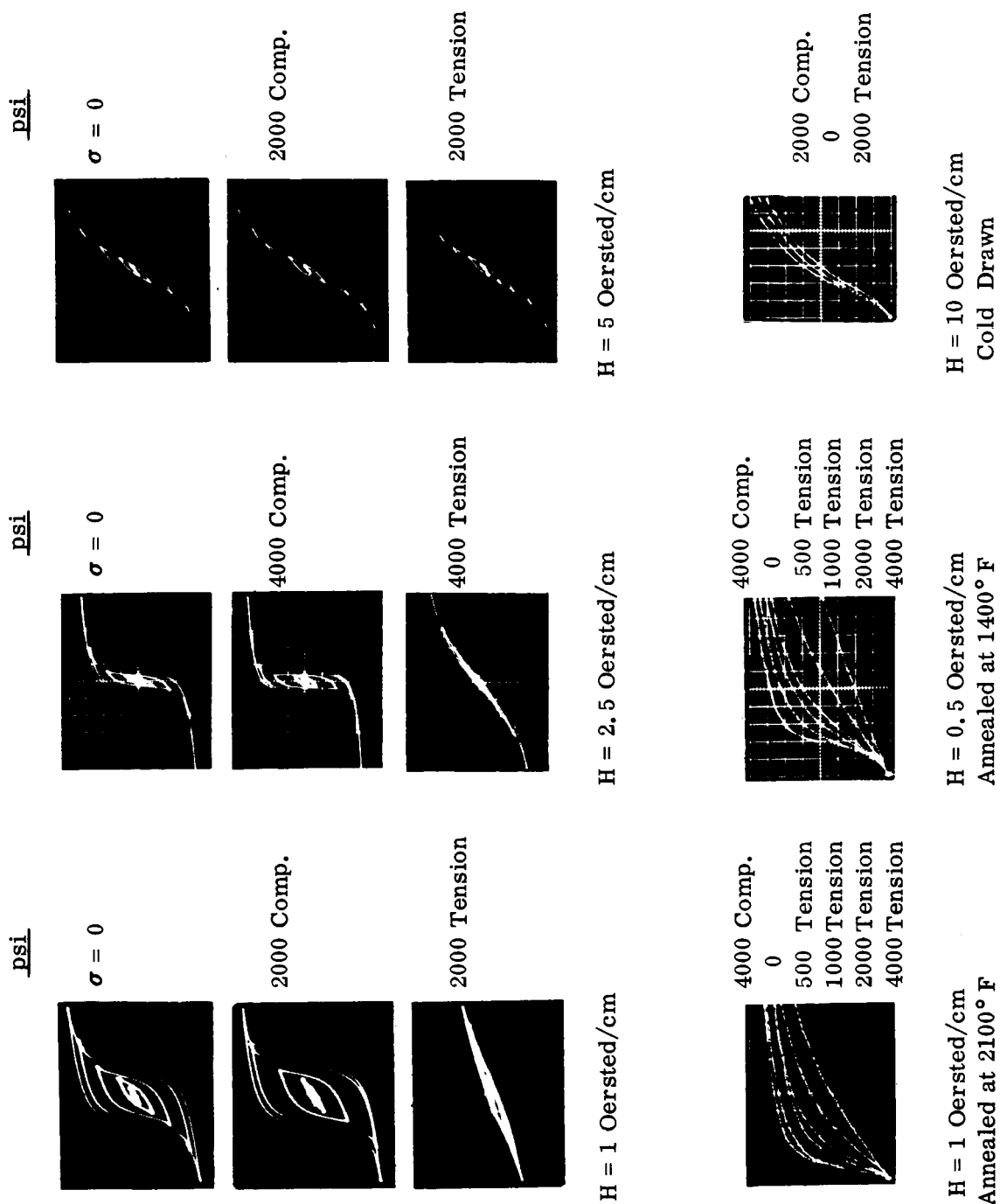


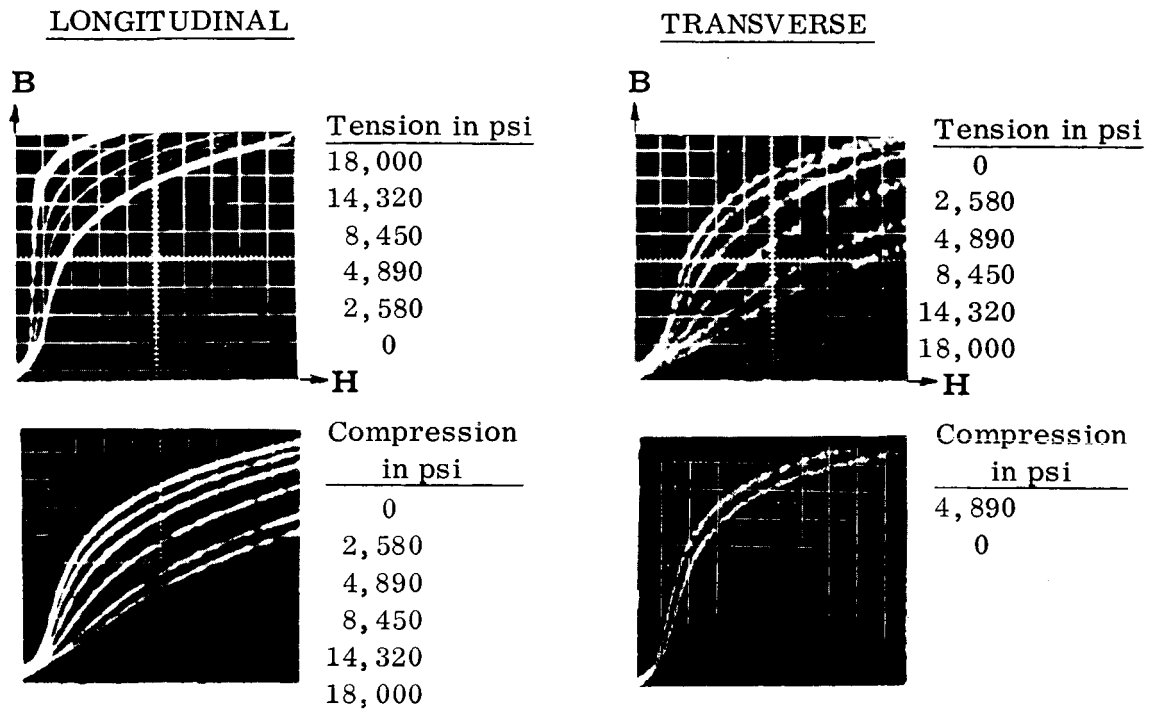
Figure 4.18. 15 cps Transverse Hysteresis and Magnetization Characteristics for 49% NiFe.

oscilloscope modulation to display the tips of the hysteresis loops as field intensity was increased from zero to H_{\max} .

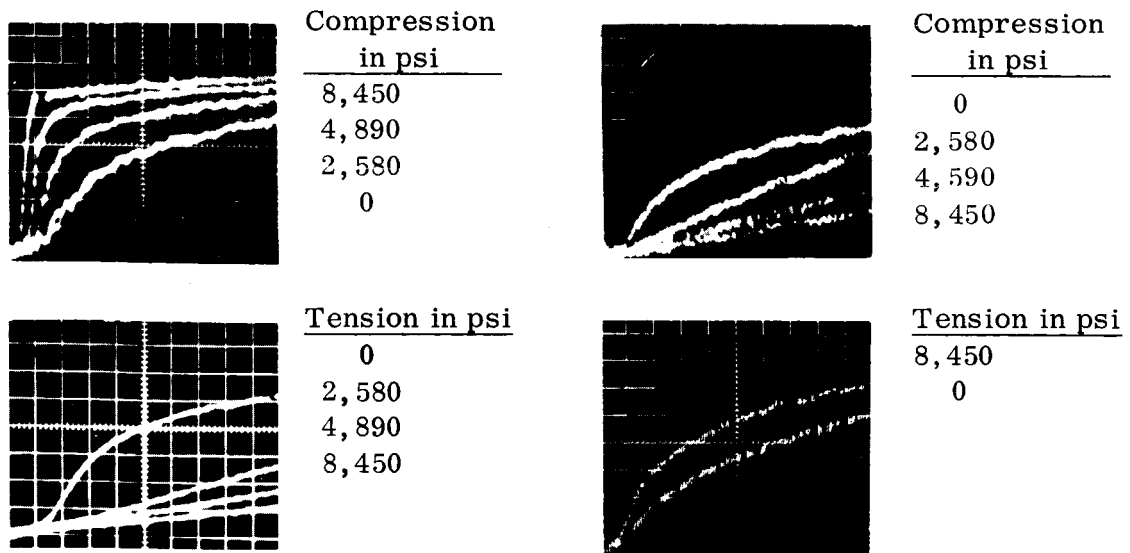
Several of the eighth-inch diameter materials samples were also tested using an alternative stressing procedure in which a tensioning line threaded through the tubular sample was used to place the sample in compression. This arrangement avoided any possibility that a portion of the sample's cross section could be in tension. No appreciable improvement in transverse strain sensitivity was observed.

Since available information on strain sensitivity is limited essentially to longitudinal characteristics, apparatus was next prepared to permit longitudinal, as well as transverse, measurements on a given material sample for cross comparison. For these measurements, the thin-wall annealed tubing used in model studies was provided with a tensioning line threaded through the tubing and arranged to place the tubing in either tension or compression. The small cross-sectional area of the tube in combination with a 10-inch sample length reduced end effects for the longitudinal measurement to the point where the demagnetizing factor could be calculated with suitable accuracy. The thin-wall tubing was prevented from buckling under compression by a stiff surrounding tube; since the possible transverse deflection was very small, transverse strains in the sample were negligibly small.

The test results shown in Figure 4.19 appear to show conclusively that the major part of the transverse strain sensitivity problem is a basic property of annealed materials and that the characteristics commonly described for longitudinal strain sensitivity cannot be extrapolated to the transverse case by merely reversing algebraic sign. The positive NiFe and the negative Ni show abnormally low strain sensitivity for compression and tension, respectively — i.e., stresses which tend to increase induction beyond the value at zero stress, regardless of whether they are compressive or tensile, are much less effective than the reverse strains which act to decrease induction. The upper curve in each of the



51% NiFe, Mill Annealed.



99% Ni, Mill Annealed.

Figure 4-19. Longitudinal vs. Transverse Strain Sensitivity of Positive and Negative Magnetostrictive Materials.

lower right-hand figures shows the highest induction obtained; with further increase of stress, induction falls below the value at zero stress. Longitudinal characteristics as shown in Figure 4.19 and the transverse characteristics of cold-drawn materials as shown in Section 4.4.2, however, have behaved normally.

4.5.1.2 EXPLANATION

As a result of those conclusions, two theories of explanation were proposed. The first assumed a preferred orientation which appears to be disproved by the X-ray diffraction patterns discussed subsequently in Section 4.5.5. The explanation which now seems most convincing is the following. For the longitudinal case, axial tension applied, e.g., to an unoriented positive material, tends to align domains axially. Magnetization by an applied axial field then involves only 180 degree rotations. The energy required to produce 180 degree rotations is less than that for rotations from the random orientations of the unstressed material. This is due to the fact that magnetostrictive strain is the same before and after 180 degree reversal, but it is changed by 90 degree rotation; a 180 degree Block wall propagates through a crystallite without gross change in the shape of the crystallite, whereas a 90 degree wall must change the overall shape of the crystallite as it progresses. The magnetization curve for the stressed material, therefore, rises more steeply than the curve for the unstressed material. By contrast, for the transverse case required in magnetoacoustic storage, a compressive stress which produces transverse domain orientation serves only to force easy directions of magnetization into the transverse plane, rather than along a given direction. The field required to produce the desired circumferential magnetization must then overcome the forces of the random two-dimensional orientations, rather than simple 180 degree rotations, and the magnetization curve of the stressed material will not rise much more steeply than the curve for the unstressed material. A proposed solution is given in Section 4.5.5.

4.5.2 B-H- σ STUDIES

The improved stress apparatus and samples of Figures 4.1 and 4.2 have provided additional significant data. The revised stress rig is provided with a pair of ball bushings to guide the drive rod instead of the single oilite bearing used originally, a precision ball bearing is used in the lever-arm pivot, the whole assembly is strengthened and the sample mounting position is maintained more accurately. The end caps bonded to the sample have flanges of diameter no larger than necessary for applying tension; compression is applied in the center of the caps so as to reduce bending tendencies to a minimum. New samples of each of the seven materials listed in Section 4.1 were assembled as shown in Figure 4.1 after being annealed in dry hydrogen for four hours at 2100°F and cooled at less than 150°F per hour.

The magnetization curves obtained for three negative materials — the two nickel samples and the 4 percent CoNi listed as samples 3, 5 and 4, respectively — are not significantly different from the initial data of Figure 4.3. With 1000 to 2000 psi of tension, samples 3 and 4 showed maximum increases in induction of 200 to 500 gauss relative to values at zero stress; sample 5 showed a decrease of 300 gauss. Data for the four positive materials are shown in Figure 4.20 to 4.23. Figure 4.20 is included to show the degree of agreement between these measurements and the data of Figure 4.5 for the NiFeCr sample which was judged the most suitable for magnetoacoustic storage in initial tests.

The 50 percent NiFe of Figure 4.21 produced no significant change in induction under compression, whereas it had dropped as much as 3000 gauss for 500 psi in initial tests under compression. It is the softest sample magnetically and shows the highest strain sensitivity for tensile stress. The dashed-line curves, which show remanence versus values of previously applied field intensity, suggest that 50 percent NiFe should provide good storage results for stress-biased operation. The application of a value of $H = 0.2$ oersted, e.g., produces a remanence with strain absent which is approximately ten times the

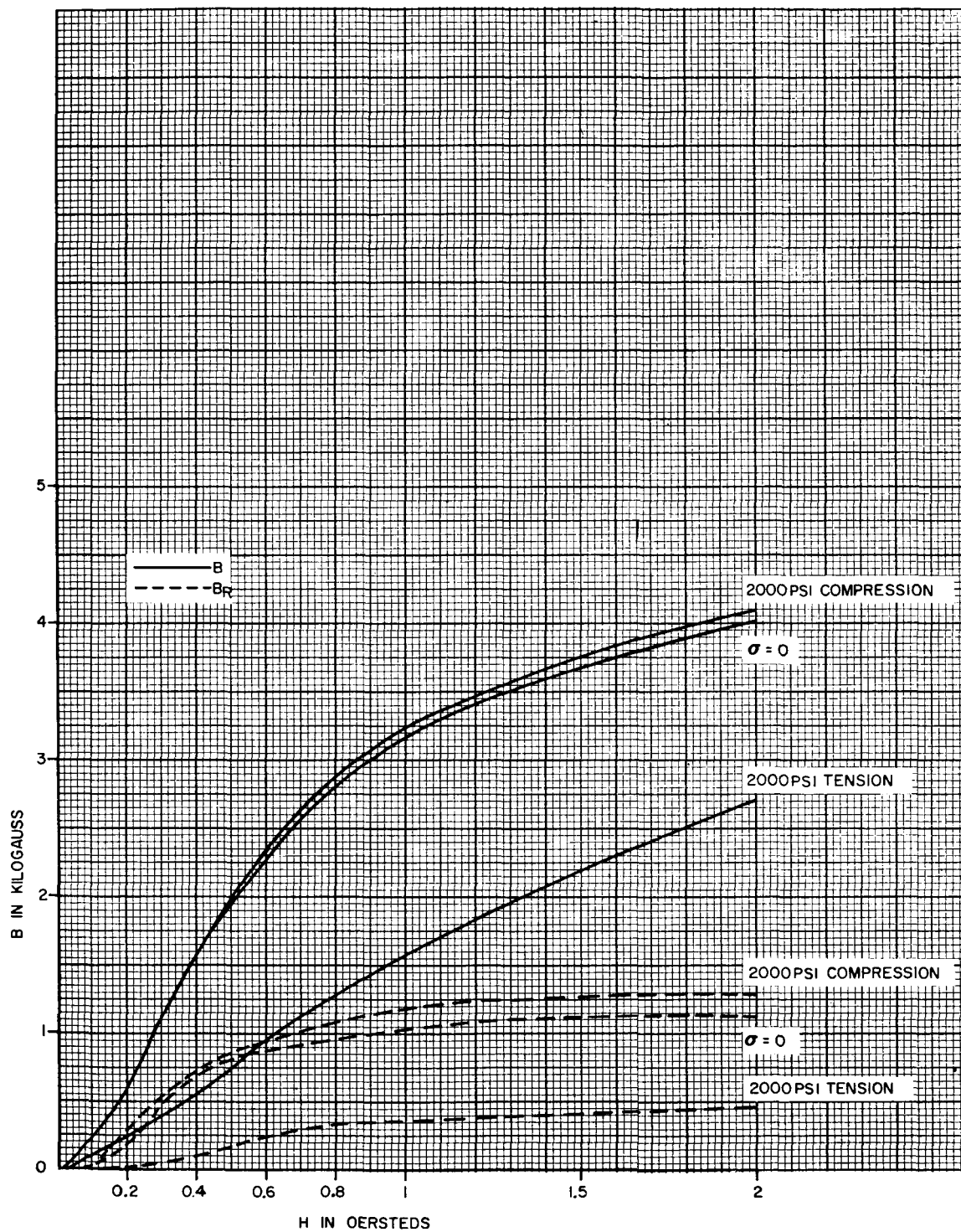


Figure 4.20. Induction and Remanence vs. Field Intensity for NiFeCr.

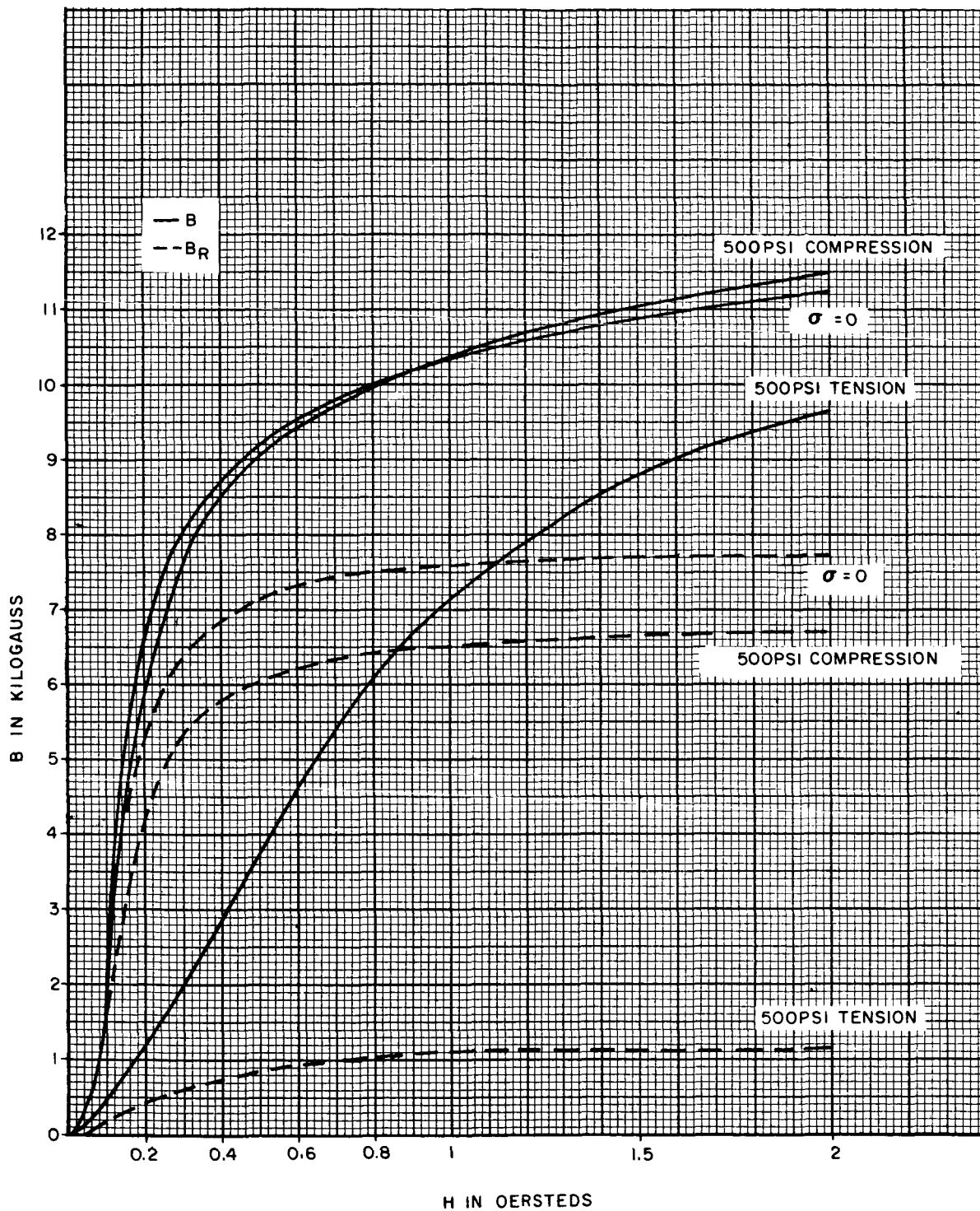


Figure 4.21. Induction and Remanence vs. Field Intensity for 50% NiFe.

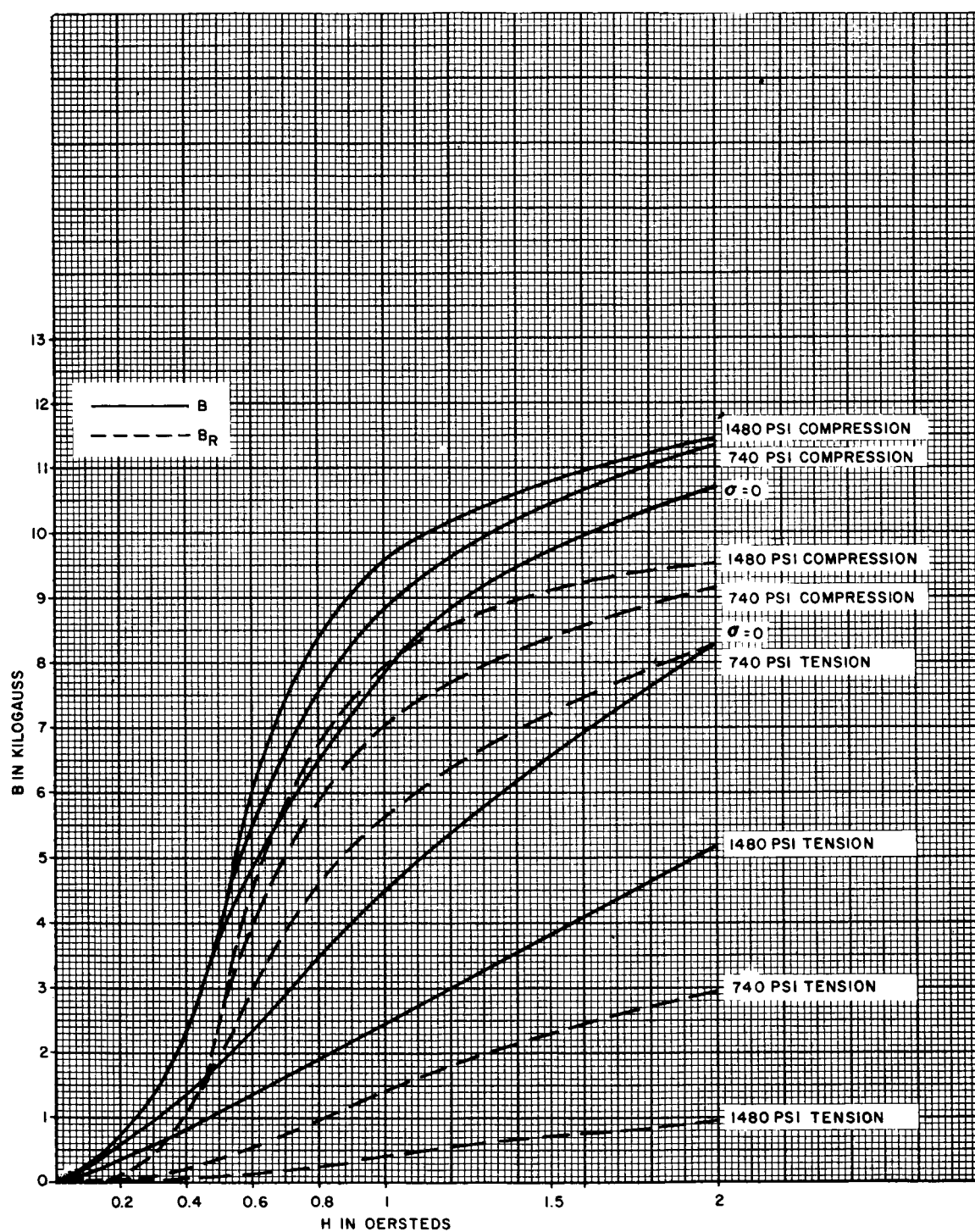


Figure 4.22. Induction and Remanence vs. Field Intensity for 49% NiFe.

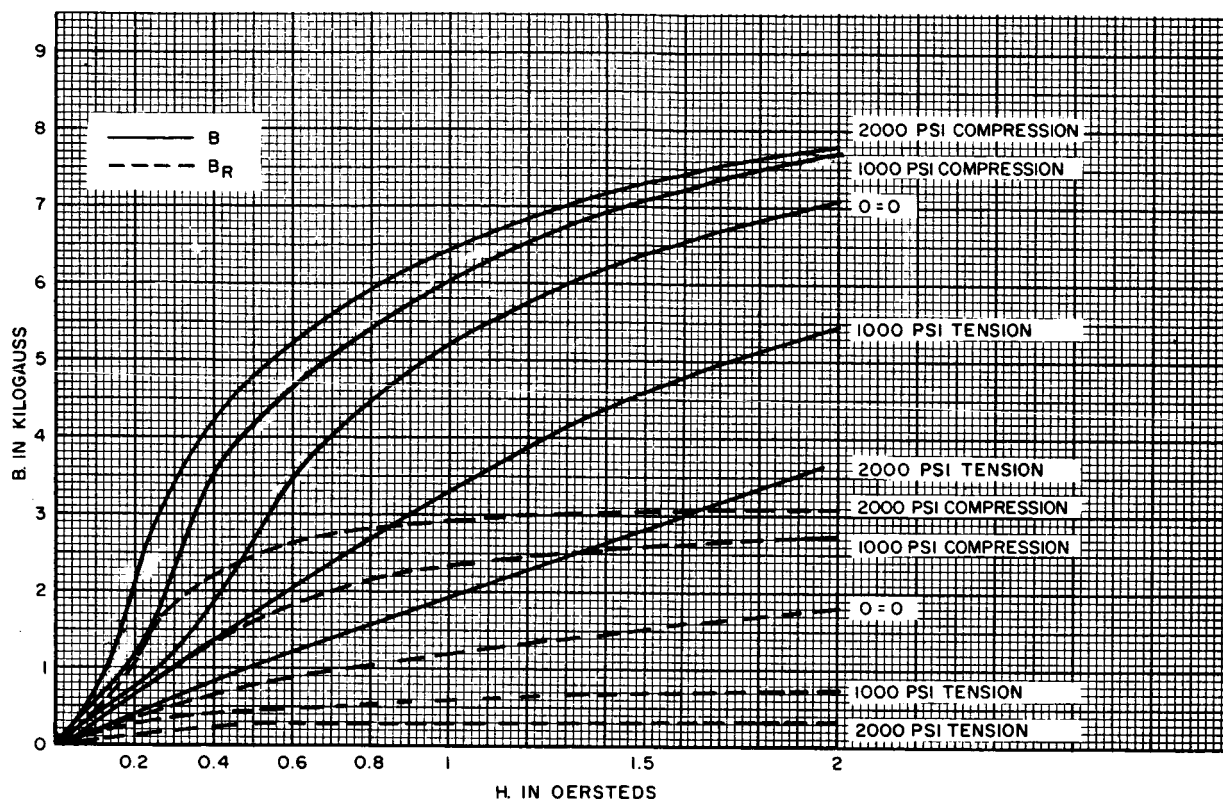


Figure 4.23. Induction and Remanence vs. Field Intensity for 70% NiFe.

remanence obtained when the sample is stress-biased. Brief tests on that sample, however, showed relatively low strain sensitivity for simulated readout. Since only limited tests on that sample have been completed, it may be possible to find more optimum operating levels in future work. Extensive measurements on the 49 percent NiFe of Figure 4.22 were undertaken first, however, because it provides a substantial increase of induction under compression, thus permitting comparative measurements for stress-biased versus zero-biased operation as discussed in the following section. The differences in the sensitivities of the 50 percent and 49 percent NiFe alloys is probably due to the fact that the latter has higher percentages of interstitial as well as substitutional impurities or additives ¹³. Analyses provided by the respective suppliers are:

	<u>C</u>	<u>Mn</u>	<u>P</u>	<u>S</u>	<u>Si</u>	<u>Se</u>	<u>Ni</u>	<u>Fe</u>
"49-FM"	0.05	1.00	-	-	0.35	0.15	49.0	Bal
52 Alloy	0.03	0.53	0.16	0.014	0.33	-	50.21*	Bal

*Ni (+Co + Cu)

4.5.3 EFFECTS OF (H, σ) SEQUENCE

As explained under 3.0 Model Studies, Part 3.7, the leading, center and trailing portions of writein pulses impose different (H, σ) sequences on the storage medium. The effect of sequence on the magnetization curves is shown in Figure 4.24. The dotted line is the magnetization curve under the usual cyclic

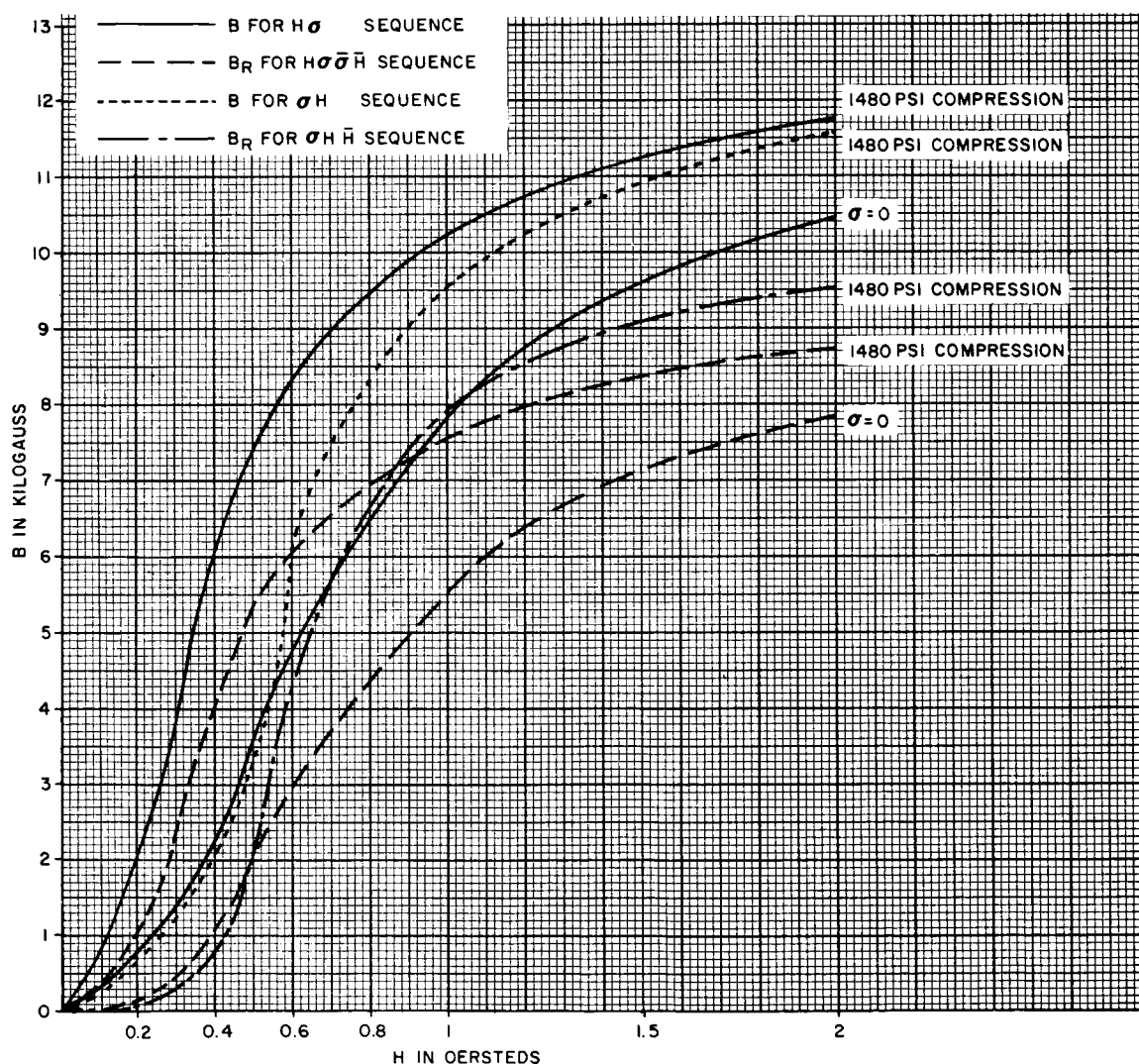


Figure 4.24. Change in Magnetization Curves with σ , H Sequence Reversal.

conditions with stress constant at 1480 psi, as previously shown in Figure 4.22. To obtain the upper solid-line curve, however, the sample was first demagnetized, the specified value of H was then applied, and stress was added finally to produce the value of induction which is plotted. The upper dashed-line curve shows the remanence corresponding to that storage sequence. The magnetization curve for zero stress applies for either the tips of the hysteresis loops under cyclic conditions or the unidirectional excursions starting from the demagnetized state. Comparison of the ratio of either B_{\max} or B_R for the stressed and unstressed conditions shows that the (H, σ) sequence of Figure 4.24 produces greatly improved results relative to the (σ, H) sequence of Figure 4.22, and this improvement occurs at substantially lower values of H .

Figures 4.25 to 4.27 for 49 percent NiFe show several factors being considered in the complex B - H - σ histories under study. A typical departure from idealized conditions is indicated in Figure 4.25 A and B. The readout ΔB 's for the two different indicated

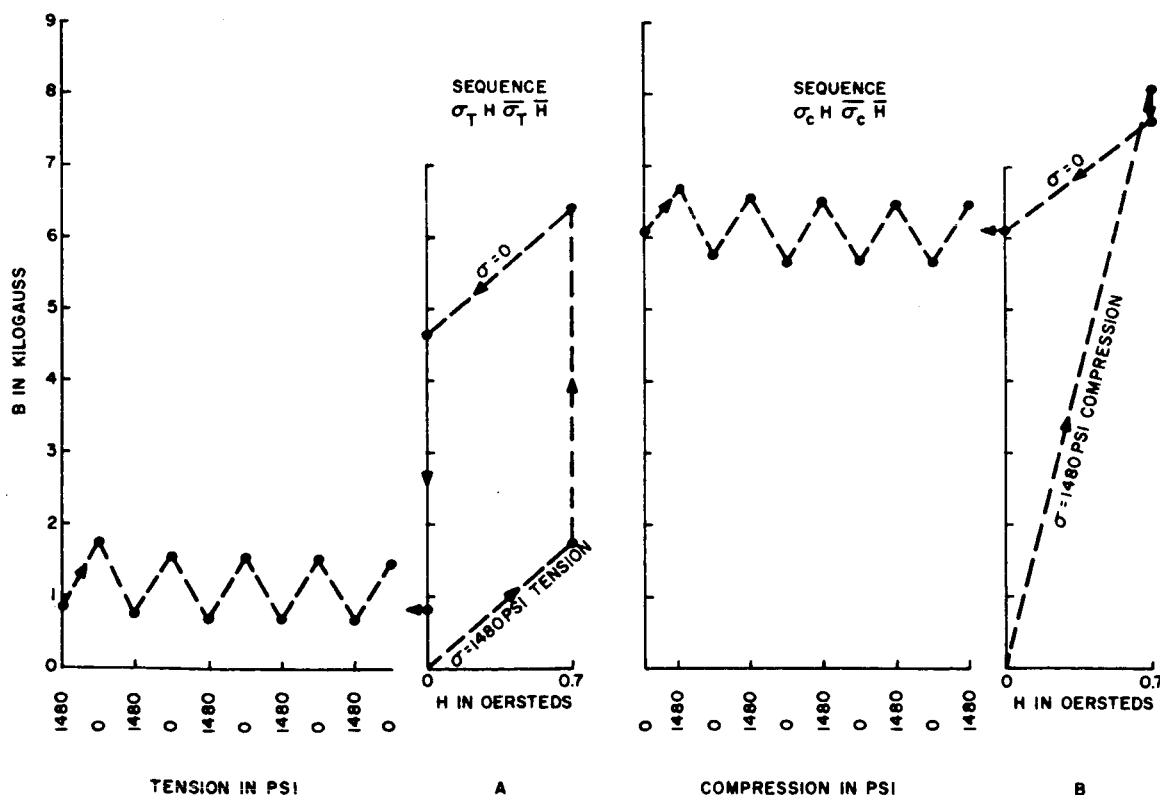


Figure 4.25. Write-Read Cycles Showing ΔB to be More Dependent on Write-In History than on Final Remanence.

writain sequences are approximately equal, but the average remanence in one case is six times that of the other. By comparison, as pointed out in Section 4.1, Bozorth and Williams¹⁴ show theoretically, for conditions of a given procedure using external polarization, that strain sensitivity is approximately proportional to induction at low values of induction and rises to a maximum at an induction equal to 0.6 of the saturation induction B_s of the material. The equal strain sensitivities of Figure 4.25 occur at approximately $0.08 B_s$ and $0.5 B_s$. Consequently, B_R data such as that shown in Figures 4.20 to 4.23 can be used only as tentative indications of magnetoacoustic storage capabilities.

Another consideration is shown in Figure 4.26. In these data for simulated stress-biased operation, the upper levels of B correspond to a ONE writain and the lower values of B correspond to a ZERO writain. As explained in Section

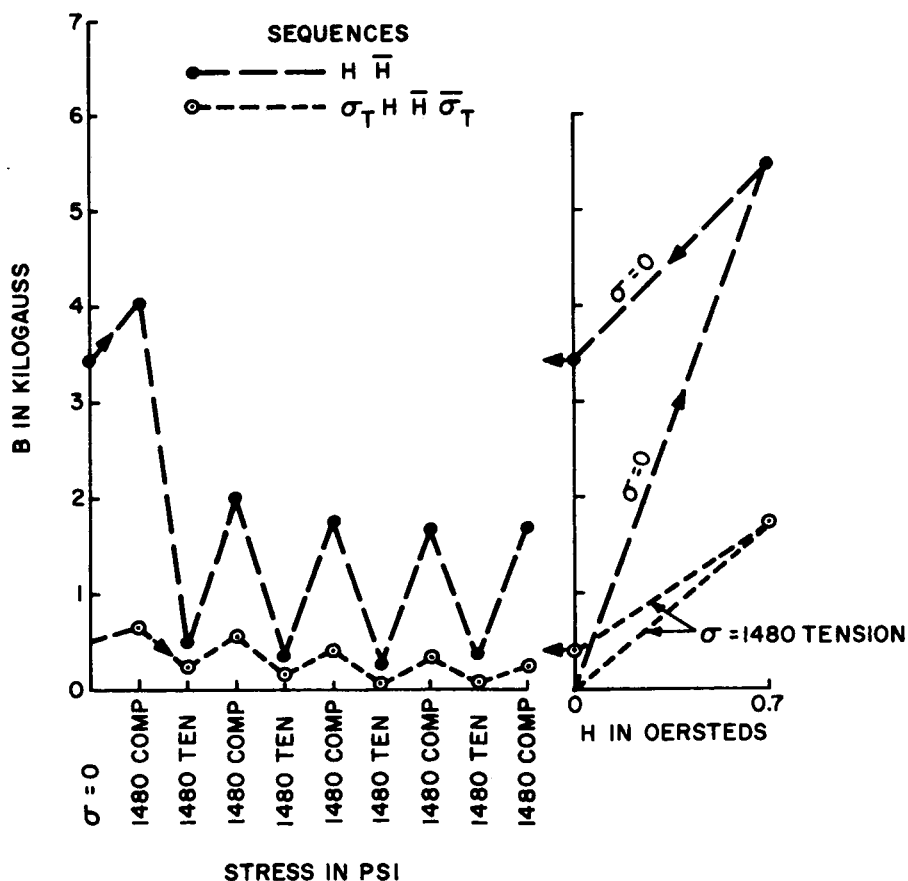


Figure 4.26. Signal and Noise Readout for Stress-Biased Writain.

4.2, S/N and output under dynamic conditions are expected to increase with the ratio of the two ΔB 's. This material when read out with $\pm \Delta \sigma$ shows a good ratio and ΔB 's which are several times larger than those of the earlier data of Figures 4.13 to 4.17. As another example, Figure 4.27 shows the largest ΔB 's obtained to date and the difference in the effects of the (H, σ) sequence for this material and one pair of (H, σ) values. It should be noted that the two curves represent ONE's recorded under different $(\bar{H}, \bar{\sigma})$ sequences, rather than representing signal and noise conditions as in Figure 4.26.

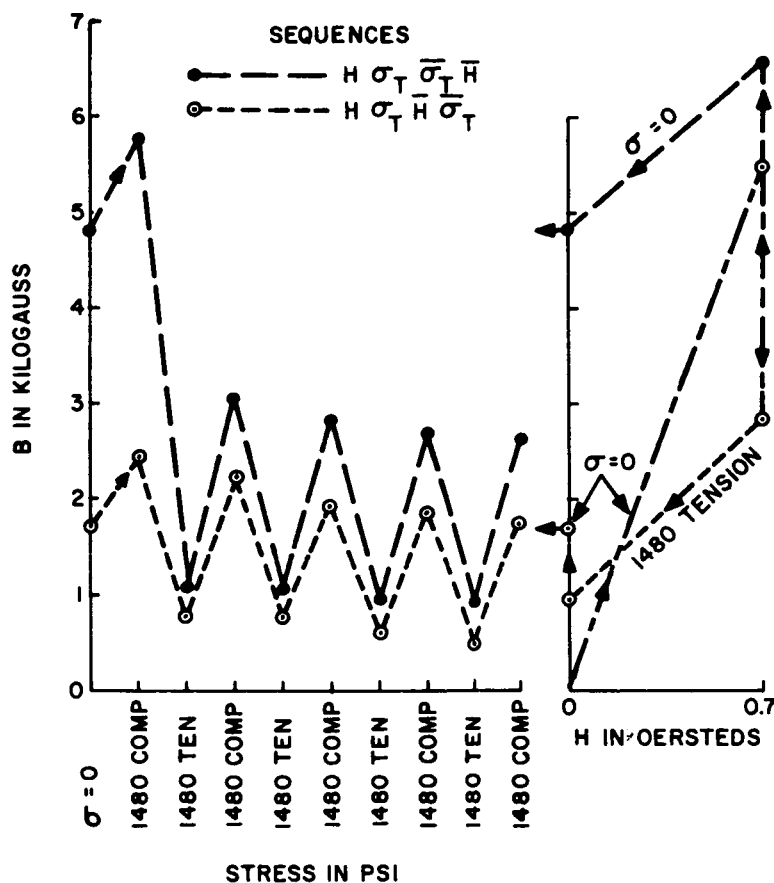


Figure 4.27. Effect of Differences in Writein Sequences using Tensile Stress.

Using procedures similar to those of Figures 4.25 to 4.27, five writein sequences simulating both stress-biased and zero-biased operation were studied in combination with two readout conditions. Data are summarized as follows for

$\Delta\sigma = 1480$ psi, where $\Delta\sigma_c$ = compressive reading stress, $\Delta\sigma_t$ = tensile reading stress and $\Delta\sigma_{ct}$ = change from compressive to tensile reading stress:

TABLE 4-1

TEST	SEQUENCE	ΔB FOR $\Delta\sigma_c$	ΔB FOR $\Delta\sigma_{ct}$	SAMPLE	H_{max}	PARAMETER SIMULATED
1	H \bar{H}	750	1400	49% NiFe	0.7	Noise
2	$\sigma_c H \bar{H} \bar{\sigma}_c$	900	1800	49% NiFe	0.7	Signal
3	H $\sigma_c \bar{\sigma}_c \bar{H}$	900	1900	49% NiFe	0.7	Signal
4	H $\sigma_c \bar{H} \bar{\sigma}_c$	900	1900	49% NiFe	0.7	Signal
5	$\sigma_c H \bar{\sigma}_c \bar{H}$	800	1850	49% NiFe	0.7	Signal
		ΔB FOR $\Delta\sigma_t$				
6	($\bar{\sigma}_t$) H \bar{H} (σ_t)	650	1400	49% NiFe	0.7	Signal
7	$\sigma_t H \bar{H} (\bar{\sigma}_t)$	250	250	49% NiFe	0.7	Noise
8	H $\sigma_t \bar{\sigma}_t \bar{H}$	850	1700	49% NiFe	0.7	Signal
9	H $\sigma_t \bar{H} \bar{\sigma}_t$	700	1300	49% NiFe	0.7	Signal
10	$\sigma_t H \bar{\sigma}_t \bar{H}$	800	1600	49% NiFe	0.7	Signal
11	H \bar{H}		100	49% NiFe	0.3	Noise
12	H $\sigma_c \bar{\sigma}_c \bar{H}$		900	49% NiFe	0.3	Signal
13	H $\sigma_c \bar{H} \sigma_c$		900	49% NiFe	0.3	Signal
14	H \bar{H}		230	70% NiFe	0.3	Noise
15	H $\sigma_c \bar{\sigma}_c \bar{H}$		210	70% NiFe	0.3	Signal

Those data lead to the following conclusions:

1. Stress-biased operation for $H = 0.7$ oersted, tests 6 to 10, gives $\Delta B_{RH}/\Delta B_{RH\sigma t}$ ratios in the range of 2.6 to 3.4 when read with $\Delta\sigma_t$, and ratios up to 6.8 for $\Delta\sigma_{ct}$, which according to Section 4.2 should provide good S/N.

2. $\Delta\sigma_{ct}$ produces approximately twice the output obtained from $\Delta\sigma_c$ or $\Delta\sigma_t$ except under the conditions of test 7, which has been confirmed in repeated tests. The ratio corresponding to this exceptional condition is 6.8.
3. Despite the good ratios of $B_{RH\sigma c}/B_{RH}$ shown in Figure 4.22 and 4.24, S/N would be poor using compressive stress and zero-biased operation at $H = 0.7$ as represented in tests 1 to 5.
4. Reduction of H to 0.3 oersted, as suggested by Figure 4.24, results in a $\Delta B_{RH\sigma}/\Delta B_{RH}$ ratio of 9, as shown in tests 11 to 13, and consequently, should provide good S/N with zero-biased operation.
5. Although the magnetization curves of Figure 4.23 for 70 percent NiFe show a substantial increase in $B_{RH\sigma}$ relative to B_{RH} at $H = 0.3$ oersted the data of tests 14 - 15 show a very poor ratio of $\Delta B_{RH\sigma}/\Delta B_{RH}$.

4.5.4 70 PERCENT NI-FE

70 percent NiFe was included in recent tests for several reasons. First, even though this is not the composition having maximum strain sensitivity, the major portion of the data presented by Bozorth¹⁵ on strain sensitivity are for 68 Permalloy; those data, despite the differences in operating conditions discussed in Section 4.1, lead to the expectation that this approximate composition should provide substantially improved results under magnetoacoustic storage conditions. Second, as shown by Bozorth and Williams¹⁴, maximum strain sensitivity varies according to

$$\Lambda_m = 0.77 \lambda_s B_s / K$$

where λ_s is the saturation magnetostriction, B_s is the saturation induction and K is the anisotropy constant for a given material. This gives a maximum in the vicinity of 60 percent NiFe when the corresponding constants for various compositions are substituted and allowance is made for the effects of internal strain anisotropy. Since inductions different than that which produces maximum Λ

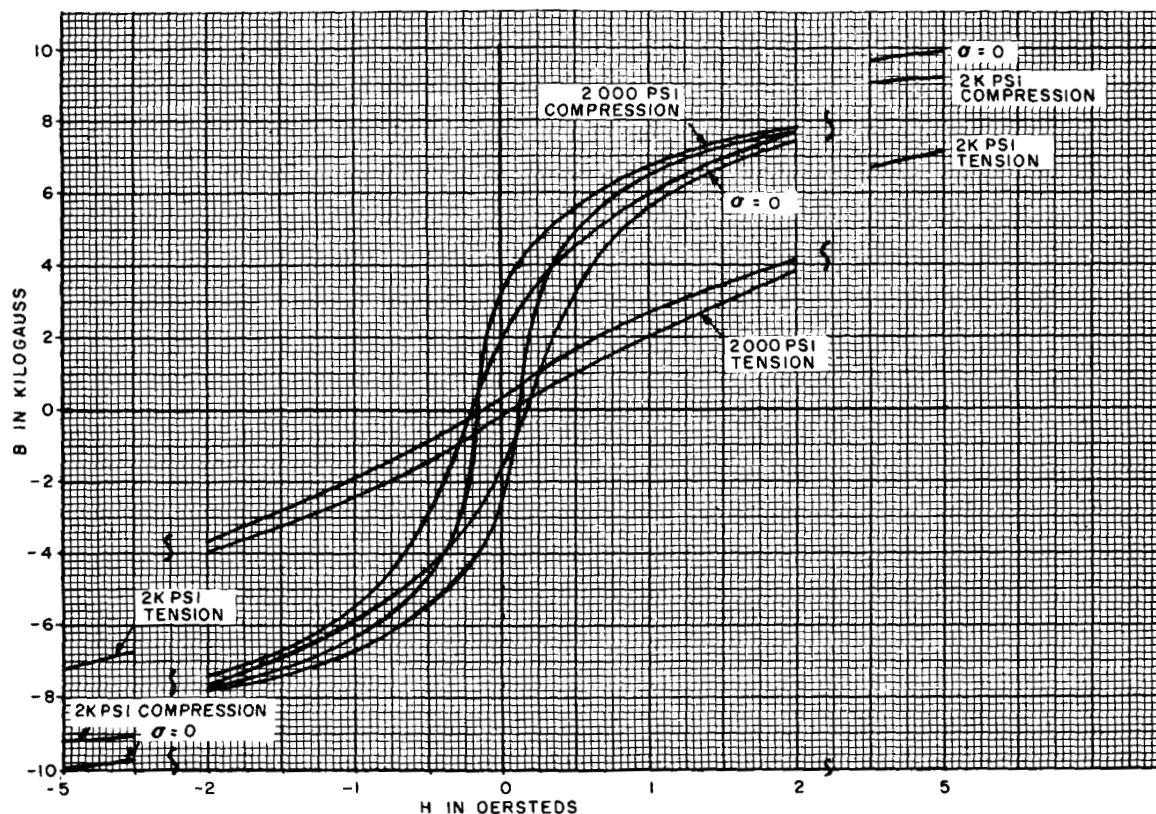


Figure 4.28. 70 Percent NiFe Hysteresis Loops.

are used in magnetoacoustic storage (in addition to other previously noted variations from the idealized case), magnetocrystalline anisotropy K may be the most significant factor. While K has a substantial value at 50 percent NiFe, it passes through zero at 70 percent NiFe. Consequently, it was expected that 70 percent NiFe, annealed to have minimum internal strains, might show improved strain-sensitivity characteristics for both read and write operations. Third, Buckley and McKeehan¹⁶ have published other data — again representing longitudinal strain sensitivity for external polarization — which indicate a further advantage for the higher nickel content. Hysteresis loops, for the series of NiFe alloys tested, show the coercive force of 65 percent NiFe to drop by a factor of seven when the material is stressed, whereas H_c for 45 percent NiFe drops only 40 percent under stress. Therefore, it appeared that 65-70 percent NiFe alloys

should provide the higher record stability needed for Mode (2) operation, as discussed in Section 2.0 and subsequently with respect to Figure 4.17 for NiFeCr.

In view of those considerations, the negative results for the sample of 70 percent NiFe tested are surprising at first. The storage properties indicated in tests 14-15, Table 4-1, are poor. Furthermore, other tests have shown that the (H, σ) magnetization curve for this sample is practically identical with its (σ, H) curve, as shown in Figure 4.23, in contrast to the large difference for 49 percent NiFe as shown in Figure 4.24. The 70 percent NiFe, however, does show the largest increase of transverse induction for any sample under axial compression and cyclic, or (σ, H) condition. Finally, the transverse hysteresis loops of Figure 4.28 for the 70 percent NiFe show only a small decrease in coercive force when the material is stressed, instead of the large factor obtained by Buckley and McKeehan for longitudinal measurements.

This latter result is probably related to the theory proposed in Section 4.5.1.2. On that basis, it is also reasonable to expect that the application of compressive axial stress to positive annealed materials should be relatively ineffective in reducing H_c . If the basic transverse strain sensitivity problem is overcome by a technique such as the orientation proposed in Section 4.5.5, it should then be found that the attributes of 70 percent NiFe, as discussed above, are advantageous for magnetoacoustic storage.

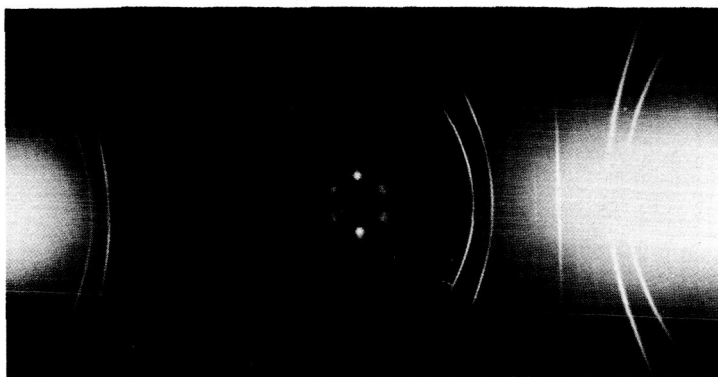
4.5.5 STORAGE MEDIA ANISOTROPY

Nickel and nickel-iron alloys having the face-centered-cubic crystal structure when cold drawn into wire or rod, generally have a double-fiber texture¹⁷ with a primary $[111]$ orientation and a secondary $[100]$ orientation parallel to the axis of drawing. The percentage of oriented crystals increases with the percentage of cold reduction in area. Drawn tubing tends to have the texture of wire or rod when its circumference and wall thickness are reduced equally and the texture of sheet when only wall thickness is reduced. For alloys in the vicinity of 50 percent NiFe, cube textured sheet can be produced in which cube faces lie parallel to the plane

of the sheet and cube edges lie parallel to the direction of rolling.¹⁸ This is accomplished by a relatively severe cold reduction during rolling, followed by high-temperature annealing. Since cube edges are the easy directions of magnetization for the 50 percent NiFe composition, such materials show easy directions of magnetization in directions parallel to, and transverse to, the direction of rolling. If the material is then given a moderate cold reduction, strains can be developed such that only the transverse direction in the bulk material is an easy direction of magnetization.

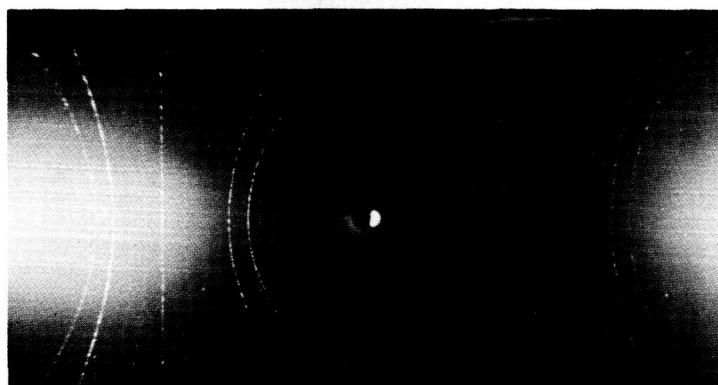
In view of that background, there appeared to be possibilities for a preferred orientation which might account for the observed difference between longitudinal and transverse magnetic characteristics. Since processing details for the material samples supplied are generally proprietary, x-ray diffraction studies were undertaken to determine what orientation was present. Each of the cold-drawn materials showed a high percentage of $[111]$ orientation, with a small percentage of $[100]$ orientation in some samples, but high-temperature annealing decreased orientation to a level which appears unlikely to explain the primary cause of difference in longitudinal and transverse characteristics. X-ray diffraction patterns for the thin-wall 51 percent NiFe used in model studies are shown in Figure 4.29 A and B for the cold-rolled and high-temperature annealed conditions, respectively. That material and the 70 percent and 50 percent NiFe alloys used in material studies, showed no observable orientation after high-temperature anneal; the 49 percent NiFe and the NiFeCr showed a definite but small $[111]$ orientation. The latter have shown better simulated storage characteristics, but present data are not believed sufficient to conclude that this is a significant correlation.

Large differences in the grain structure which developed during high-temperature anneal were observed in the x-ray diffraction data. The increase in grain size indicated in Figures 4.30 A and B is representative of the smaller changes observed in the materials studied. The x-ray diffraction data were followed up with photomicrographs of several samples for two reasons. First,



A.

Plate 9 (Cold Rolled).



B.


Plate 13 (Annealed).

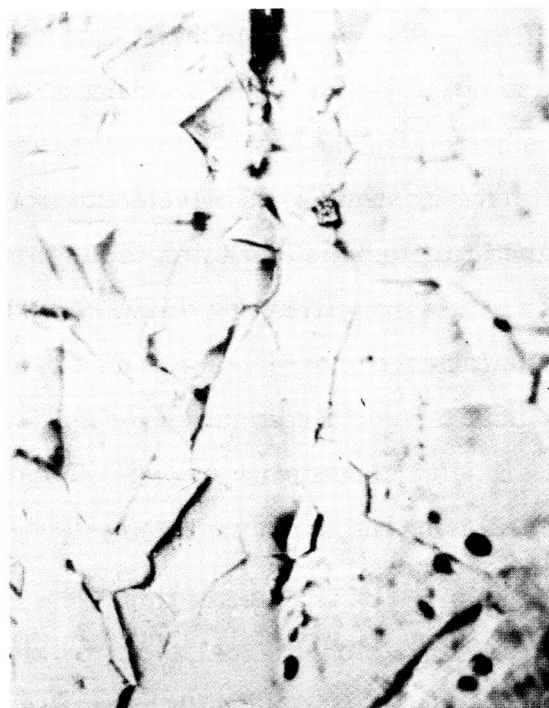
Figure 4.29. X-Ray Diffraction Patterns for Thin-wall 51% NiFe.

grain size is an important factor limiting the upper frequency response of polycrystalline materials. The anisotropy of the elastic constants in grains causes a large loss ¹⁹ from the scattering of sound when wavelength is in the order of grain size. Second, non-magnetic inclusions elongated in the direction of drawing could cause the transverse magnetic properties of a sample to be substantially poorer than its longitudinal properties — particularly in annealed materials for which internal strains tend to be a less dominant factor. Figures 4.30 A and B for NiFeCr, before and after annealing, respectively, were obtained after surfaces had been lapped and etched using the same procedures. From study of the photomicrographs for several materials, it was concluded that elongated inclusions do not appear to be responsible for the observed difference in the longitudinal and transverse properties of annealed materials. Also noteworthy is the observation that the average grain size of the annealed NiFeCr is somewhat smaller than the 100-200 microns for which Mason ²⁰ gives an upper response limit of 4 megacycles.



Cold Rolled

Scale:  50
microns



Annealed

Figure 4.30. Photomicrographs of Grain Structure for NiFeCr.

Annealed samples of the 70 percent NiFe and 49 percent NiFe materials showed grain sizes several times larger. Further data will be required, however, to determine whether those orientational results are consistently representative of relative grain sizes.

The primary conclusion of this work is that the discussion of Section 4.5.1.2 offers the most promising answer to the transverse strain sensitivity problem. On that basis, a medium having controlled anisotropy is needed — i.e., one having a circumferential direction of easy magnetization and a radial direction of difficult magnetization. This should be possible with drawn tubing using procedures outlined in the first paragraph of this section, but the shape anisotropy of thin films may provide a more direct approach.

4.5.6 THIN FILMS

The major emphasis of the studies of Section 4.5 was placed on fully annealed materials. The increased acoustical attenuation resulting from increased grain size was disregarded because of the expectation that ultimate performance will be achieved with an optimized thin-film storage material deposited on a low-loss core material. Thin films now appear to offer a means of improving the sensitivity or efficiency of the basic low-frequency storage technique as well as the well-known advantages of lower losses for high-frequency operation. They also offer a convenient means of testing the theory proposed to explain the observed behavior of transverse strain sensitivity for drawn materials. If confirmed, a basis would exist also for the improvement of drawn tubing or clad materials which then may prove to be competitive with thin films for applications requiring only moderate information densities and operating speeds. Comparative media processing costs, uniformity, efficiency, and output levels also require evaluation.

Confirmation will require a series of samples of thin films in graduated thickness and a configuration permitting longitudinal and transverse strain sensitivity measurements similar to those described with reference to Figure 4.19. For these tests the object will be to determine the film thickness for which radial

components of easy magnetization are sufficiently suppressed to cause the desired enhancement of circumferential strain sensitivity; random orientation in the cylindrical surface is desired. One electrodeposited NiFe thin film was prepared and tested at zero stress. The hysteresis loops of Figures 4.31 A and B for the hardest and easiest directions of magnetization, respectively, show a small anisotropy caused by earth's field which was not nulled for this initial film. Coercivity averages 1.6 oersteds. Estimated composition, based on electro-deposition current density, is approximately 60 percent NiFe.

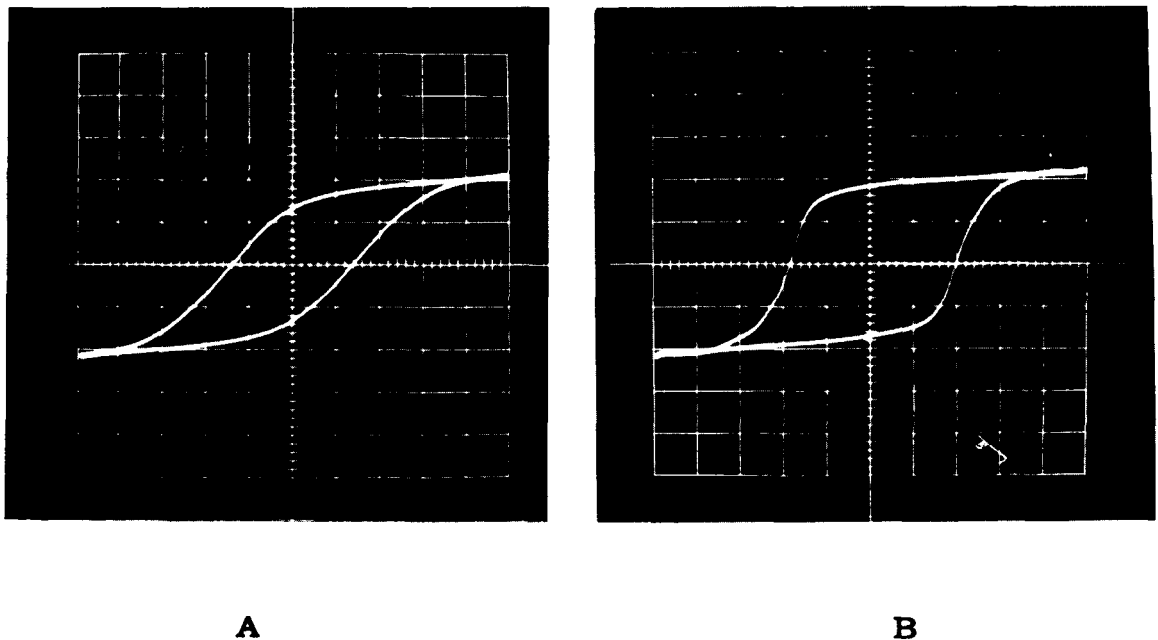


Figure 4.31. NiFe Thin-film Hysteresis Characteristics.

5.0 CONCLUSIONS

1. Practicable performance for small memories can be obtained from a storage line of commercially available, mill-annealed, "52 alloy" tubing having an OD of 15 mils and a wall thickness of 2 mils. Alternative characteristics for this line under Mode (1) operation, using zero and plus polarizing fields, are as follows:

- a. Simple magnetostrictive transducers, utilizing reflections from undamped ends of the line, can be used to reinforce the stress pulse to a level suitable for writein. The resulting continuously-circulating, high-level stress pulse permits a system of simple construction which is functionally equivalent to a continuously rotating drum memory. The transducer is a solenoid surrounding a short section of the storage medium, thus avoiding constructional problems associated with the coupling of alternative transducers. With 3-microsecond pulses, 13 db S/N can be obtained for a single writein, or 17 db S/N for repetitive writein. The latter may be applicable to library-type storage; a usable S/N for a 1-microsecond pulse could probably be obtained by reducing tubing OD to 5 mils.
- b. Piezoelectric transducers, based on interpretation of data for the horn-coupled model, can provide sufficient stress level for obtaining 13 db S/N with direct drive and a 3-microsecond pulse. Under this condition, a large number of repetitions of polarizing field during writein, such as would occur in filling a line with data, reduces the S/N for initially stored pulses to 8 db. This effect can be avoided by Mode (3) operation in which data are applied to the transducers, and all data are standing on the line when a single application of polarizing field effects writein. With a 1:10 pressure transforming horn, S/N was 12 db and 20 db for 1- and 3-microsecond pulses respectively.
- c. Mode (2) operation, using plus and minus writein polarizing fields, offers

the advantages of random-access writein within a given line and avoidance of need for the special erase operation involved in Mode (1) operation. Early dynamic data and extensive static materials data led to the conclusion that Mode (2) operation would require special materials processing and/or higher transducer and polarizing-field powers than Mode (1).

2. The estimated resolution limit is approximately one microsecond for conditions of direct piezoelectric drive, Mode (1) operation and unoriented "52 alloy" tubing having a wall thickness of one mil, the minimum thickness available in combination with an OD of 5 to 10 mils. The corresponding packing density of 6 bits per linear inch for return-to-zero storage would require, e.g., that lines be packaged on a 10-mil center-to-center spacing in order to store 10^8 bits in one cubic foot.

3. Orientation of storage media, on the basis of proposed theory, appears to promise an order-of-magnitude increase in strain sensitivity. The resulting relaxation in driving requirements is expected to permit an increase of usable resolution to approximately 0.5 microsecond using oriented drawn materials under Mode (1) operation. The development of thin-film media will be required for higher information packing densities.

4. Additional results from static and low-frequency studies of 8 alloys of Ni, Fe, Co, and Cr are as follows:

- a. Anneal at 2100°F , in general, raises strain sensitivity and reduces coercive force by roughly an order-of-magnitude relative to values for cold-drawn samples. Acoustical attenuation becomes excessive in homogeneous lines after the high-temperature anneal, but results are believed applicable to thin films deposited on a low-loss core. An anneal at 1600°F has provided a practicable compromise for homogeneous lines of 51 percent NiFe.
- b. Repetitive (non-destructive) readout causes only a tolerable loss of signal level in annealed materials as well as cold-drawn materials.

- c. Annealed, drawn tubing, in general, shows very low transverse strain sensitivity for stresses which tend to raise induction above the value for zero stress. The use of a tensile stress bias with media of positive magnetostriction is one means for utilizing the higher strain sensitivity of annealed commercial materials.
- d. Performance criteria developed for Mode (1) operation show S/N and output level to be functions of the ratio of the strain sensitivities for the ONE and ZERO remanence values. A ratio of 2, e.g., should provide 10db S/N if media uniformity varies ± 10 percent. Each of the three annealed samples, Ni, 49 percent NiFe and NiFeCr, which were tested under simulated stress bias showed ratios of 2 and better for a stress of 1000 psi in initial tests. Subsequent work concerning the effects of (H, σ) sequence, and proposed oriented media, promise comparable or improved ratios without the use of stress bias.
- e. Explanation of the effect noted in (c) suggests that a storage medium having anisotropy which suppresses radial directions of easy magnetization should show transverse strain-sensitivity characteristics similar to the better known, more favorable, longitudinal characteristics.
- f. Changes in the sequence in which the stress and the polarizing field are applied cause major changes in subsequent readout strain sensitivity for a given value of remanence. Stresses in the direction tending to increase induction beyond the value at zero stress do result in substantially increased transverse strain sensitivity when stress is applied after the polarizing field. The fact that this sequence does occur at the trailing edge of recorded pulses under dynamic conditions may explain the degree of success achieved in model tests without using strain bias. Substantially better results should be obtained with transverse characteristics which are comparable to typical longitudinal characteristics.

- g. Seventy percent NiFe showed the best increase in transverse induction of any sample when subjected to axial compression, but simulated write-read results were poor.
- h. The NiFeCr sample showed the best ability to resist erasure during application of the reverse polarizing field required for Mode (2) operation in simulated tests.

6.0 RECOMMENDATIONS

1. The modest one-microsecond pulse resolution, which was demonstrated, represents a basic capability for storing 10^6 bits, e.g., in a 2.6-inch cube using presently available materials. Practical realization will involve:

- a. Demonstration that one-microsecond resolution can be obtained with direct piezoelectric drive, instead of horn coupling, when a finer storage line is substituted.
- b. Development of means for assembling, matching and bonding the fine lines to the driver, and means for making electrical connections, without introducing excessive reflections.
- c. Means of stacking lines on 10-mil center-to-center spacings.
- d. Evaluation of storage line uniformity.
- e. Evaluation of overall power requirements.

It is recommended that efforts be undertaken to demonstrate the overall capabilities with a feasibility model consisting of a small number of matrixed short lines of "52 alloy" tubing having a 5-mil OD and a 1-mil wall thickness or solid wire of approximately 1-mil diameter. The development of matching, bonding and support techniques are expected to be the major problems; achievements will be applicable also to the following advanced approaches.

2. A thin-film storage medium deposited on a low-loss core offers potential improvements in speed and linear data densities of at least an order of magnitude. The high volume density proposed in item 1 above results primarily from the high density of line stacking anticipated. For applications requiring high-speed sequential readout of long data blocks of the order of 100 bits or more, the higher linear density along a single line, as promised by thin-film approaches, is needed. Consequently, it is recommended that a suitable combination of low-loss core and thin film be developed, considering initially alloys in the 50 - 70 percent NiFe range.

3. An oriented storage medium is proposed for increasing transverse strain sensitivity, thus substantially reducing drive requirements as well as limitations on usable resolution. The use of thin films for initial study is recommended. Basic results may then be adapted to drawn media if considerations such as processing costs or media uniformity are found to favor drawn media for small memories.

4. Continued study, which is believed applicable to both item 1 and item 2 approaches, is needed to further understanding of the following:

- a. The effects of strain and polarizing-field sequences.
- b. Anticipated, but unproved, sensitivity and stability advantages for 70 percent NiFe.
- c. The exceptional ability of NiFeCr to tolerate reverse polarizing fields, in Mode (2) operation, without erasure.
- d. The high strain sensitivity indicated by magnetization curves for "52 alloy" versus its poor performance in the simulated write-read cycle.
- e. The fact that two annealed materials having small [111] orientation showed substantially better storage characteristics than two other annealed materials having no observable orientation.
- f. The relative advantages of operating Modes (1), (2) and (3) following further improvements in basic storage characteristics resulting from orientation and changes in media composition.

APPENDIX I REFERENCES

SECTION 2.0

1. R. C. Williams, "Theory of Magnetostrictive Delay Lines for Pulse and Continuous Wave Transmission," Transactions of IRE-PGUE, February 1959.
2. A. Rothbart and L. Rosenberg, "A Theory of Pulse Transmission Along a Magnetostrictive Delay Line," Transactions of IRE-PGUE, December 1957.
3. T. B. Thompson and J. A. M. Lyon, "Analysis and Application of Magnetostrictive Delay Lines," Transactions of IRE-PGUE, August 1956.
4. A. Gabor, "High-density Recording on Magnetic Tape," Electronics, October 16, 1959.

SECTION 4.0

1. R. M. Bozorth, Ferromagnetism, D. Van Nostrand, 1951, pp. 595-712.
2. R. M. Bozorth and H. J. Williams, "Effect of Small Stresses on Magnetic Properties," Review of Modern Physics, Vol. 17, No. 1, January 1945, p. 73.
3. Ibid., pp. 77-79.
4. O. E. Buckley and L. W. McKeehan, "Effect of Tension Upon the Magnetization and Magnetic Hysteresis in Permalloy," Physical Review, Vol. 26, 1925, pp. 265-268.
5. R. M. Bozorth, op. cit., pp. 634-660.
6. R. E. Fischell, "Effects of Transverse Compressional Stress on Magnetic Laminations," AIEE Transactions Part I, Communications and Electronics, Vol. 74, 1955, pp. 190-191.
7. R. M. Bozorth and H. J. Williams, op. cit., pp. 75, 78.
8. C. A. Clark, "Improved Nickel-Base Alloys for Magnetostrictive Transducers," Jour. of the Acous. Soc. of Amer., Vol. 33, No. 7, July 1961, pp. 930-3.

9. R. M. Bozorth, op. cit., p. 601.
10. Ibid., pp. 597, 607.
11. H. P. Epstein and O. B. Stram, "A High-performance Magnetostriction Delay Line," Transactions of IRE-PGUE, August 1957, pp. 10-12.
12. R. M. Bozorth, op. cit., p. 613.
13. F. Brailsford, Magnetic Materials, John Wiley and Sons, 1960, p. 72.
14. R. M. Bozorth and H. J. Williams, op. cit., p. 77.
15. R. M. Bozorth, op. cit., pp. 595-614.
16. O. E. Buckley and L. W. McKeehan, op. cit., pp. 267-8.
17. C. S. Barrett, Structure of Metals, McGraw Hill Book Co., Inc., 1952, pp. 442-509.
18. F. Brailsford, op. cit., p. 129.
19. W. P. Mason, Physical Acoustics and the Properties of Solids, D. Van Nostrand, Inc., 1958, p. 206.
20. Ibid., pp. 130, 206.